Prediction and Suppression of Chaotic Instability in Brake Squeal

Paul Anthony Meehan (meehan@uq.edu.au)
University of Queensland

Research Article

Keywords: brake squeal, chaotic instability, Hopf bifurcation

Posted Date: May 10th, 2021

DOI: https://doi.org/10.21203/rs.3.rs-494228/v1

Version of Record: A version of this preprint was published at Nonlinear Dynamics on November 1st, 2021. See the published version at https://doi.org/10.1007/s11071-021-06992-1.

PREDICTION AND SUPPRESSION OF CHAOTIC INSTABILITY IN BRAKE SQUEAL

Paul A. Meehan [1,*]

[1] The University of Queensland, Brisbane, Australia

[*] E-mail: meehan@uq.edu.au

Abstract: Chaotic instability in a vibration phenomenon, known as brake squeal, is investigated including the combined effects of falling friction and mode coupling. Brake squeal is a high-pitched noise that occurs sometimes when a vehicle is decelerated using disk brakes. The equations of motion for the two dominant coupled modes of the brake system reduce to two autonomous coupled nonlinear second order systems. The mode coupling instability via friction causes limit cycle behaviour via a Hopf bifurcation. This limit cycle is shown to break up into chaotic motion characterised by a phase space with an approximate one-dimensional attractor, similar to that found in a forced dry friction oscillator. For the first time, conservative analytical conditions for brake squeal chaos are developed and verified numerically over a range of sprag angles and brake pressures for fundamental and real brake systems. The predictive model is then used to identify and quantify means to suppress brake squeal chaos to unlikely, excessive friction levels. The results provide predictive insight into conditions under which brake squeal chaos occurs and its suppression.

Keywords: brake squeal, chaotic instability, Hopf bifurcation.

1. Introduction

Brake squeal is an annoying high-pitched tonal noise that occurs during braking of a vehicle using disk brakes. For the automotive and railway industries, this causes undesirable noise and vibration resulting in excessive customer complaints and warranty costs [1]. In general, brake squeal occurs due to a friction induced instability of one or more brake system modes of vibration that grows to a nonlinear limit cycle and/or bounded chaotic oscillations. An understanding of the occurrence of brake squeal chaos requires insight into the underlying mechanisms of it's instability. There have been several specific mechanisms of brake squeal investigated, as reviewed in [2], including; falling friction, spragging [3][4] and mode coupling [8][9].

Spurr [3] first suggested the 'sprag-slip' mechanism for the instability of brake squeal. He found a semi-rigid strut inclined to a moving surface could 'sprag' or dig into the moving surface and then dynamically slip based on the static friction and the sprag angle [4]. This was verified using 'pin on disc' testing [5] and beam-on-belt numerical simulations [6] including beam elasticity and finite thickness. Fieldhouse [1],[7] applied sprag-slip theory to a real brake system geometry to identify the sprag angle and determine how the position of the dynamic centre of pressure of a brake pad affects squeal [20]. North [8] identified the mechanism of mode coupling in automotive brake squeal, analogous to 'binary flutter', and Hoffman [9] performed a reduced model numerical analysis to provide important mechanistic insight and the effects of damping [10][21]. The relationship between spragging and mode coupling was solidified in [18] where spragging of the dynamic modes was identified as an important condition for mode coupled squeal [18]. Complex eigenvalue analysis can be used to numerically predict brake squeal mode coupling in complex geometries, although recently an analytical solution for a reduced two mode system has been identified [18]. Simplified test rig results have confirmed that mode coupled squeal primarily occurs due to two distinct modes with closely spaced natural frequencies [22]. In full brake assemblies squeal frequencies were found to typically vary from 2-15kHz due to a combinations of rotor circumferential in-plane modes, diametric out-of plane modes and radial in-plane modes [11]-[17]. A comprehensive FEA and experimental investigation of a 3kHz squeal in a real full brake system, by Park [15], is used for verification in this paper. Recently, a closed form prediction for the occurrence, growth and amplitude of brake squeal was identified [18], but chaos was not investigated.

Oberst and Lai [25] provided a comprehensive review of research into chaotic instabilities in brake squeal and related friction coupled systems. Experimental and numerical chaos due to dry friction instability was identified by Feeny and Moon [26] in a fundamental forced oscillator. The chaotic attractors were found to have common features despite the different friction laws used. More specifically, in a simplified 2 degree of freedom brake pad and disk system, Shin et al [36] performed a numerical stability analysis and showed squeal limit cycle attractors in phase space, dependent on the closeness of the modes and stabilizing or destabilizing damping. Large nonlinear chaotic-like motion was also noticed following a period doubling route, however the motion was not conclusively identified [37]. In [40], nonlinear time domain analysis of a brake model showed intermittent bursts of very high amplitude vibrations via an intermittency route to chaos. Chaos inherent to a stick-slip oscillator was quenched using large amplitude dither in Feeny and Moon [41] and Lin et al [38] numerically identified and controlled brake disk squeal using state feedback control. Conversely chaotic instability in a full-scale brake system was confirmed numerically and experimentally and the transition from a limit cycle to an unstable torus attractor [25] was quantified. In addition, a novel method to estimate Lyapunov exponents from brake

squeal measurements was demonstrated in [39] using noise in a Eckmann-Ruelle statistical procedure and showed quasi-periodic or slightly chaotic behaviour.

Although this previous research has numerically or experimentally identified chaotic instability in brake squeal, no closed form analytical predictive criteria for its onset have been developed. Therefore, in addition, there has been no predictive insight to analytically quantify measures to avoid brake squeal chaos. In addition, the combined mechanisms of mode coupling and falling friction have not been specifically investigated. To address this, the present research is focused firstly on the predictive identification and quantification of chaotic instabilities in brake squeal under 'falling friction' and mode coupled conditions. Subsequently the model is used to predict and quantify means of eliminating chaos in brake squeal. The major contributions include:

1. Closed form analytical predictions and quantification of chaotic instability in brake squeal, under mode coupling and falling friction mechanisms, validated with numerical simulations and nonlinear dynamics tools.
2. Further insight into the conditions associated with brake squeal chaotic instability.
3. Analytical prediction to identify and quantify parametric control methods to suppress brake squeal chaos.

This paper will first describe the reduced two mode brake squeal model consisting of two autonomous coupled nonlinear second order systems with a nonlinear friction law. Closed form analyses to predict the local instability occurrence, growth and limit cycle amplitude of brake squeal are then reviewed and developed. Conservative analytical criteria for the onset of brake squeal chaos are then derived. Numerical simulations are then performed and quantitative nonlinear dynamics tools (including Poincare maps and Lyapunov exponents) are used to identify chaotic instability onset and compared with the analytical necessary criteria in simplified fundamental and real brake model cases. The criteria are used to efficiently predict a range of typical brake parameters under which chaotic squeal could occur. The criteria are then used to efficiently investigate a range of typical brake parameters under which brake squeal chaos can be eliminated or suppressed to unrealistically high, static friction levels.

2. Methodology

A reduced two mode brake squeal model consisting of two autonomous coupled nonlinear second order systems with a nonlinear friction law is first described [18]. Closed form analyses to predict the local instability occurrence, growth and limit cycle amplitude of brake squeal are then described in section 2.2. These are then used with Lyapunov exponent theory to develop conservative analytical criteria for the onset of brake squeal chaos in 2.3.

Figure 1 describes the fundamental mechanical interactions causing brake squeal limit cycle oscillations and noise.

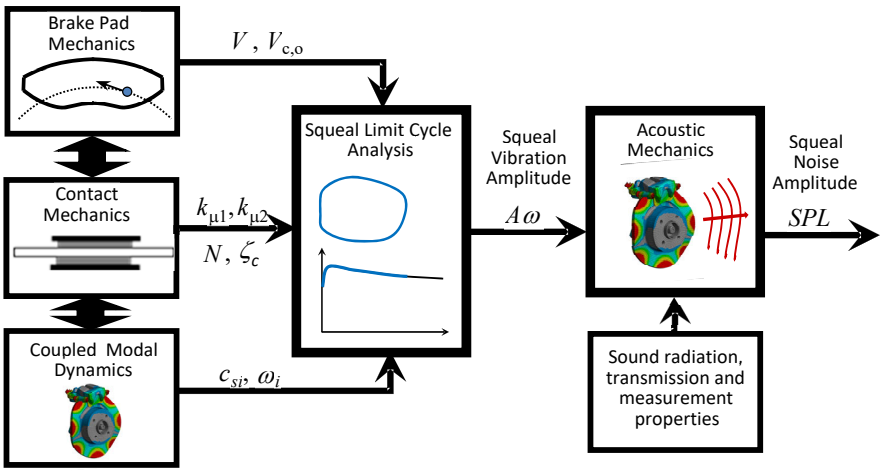

Figure 1 *Conceptual Model of brake squeal noise. [18].*

Essentially the contact mechanics couples the brake pad mechanics and coupled modal dynamics of the brake pad and rotor system. The brake pad mechanics determines the centre of pressure of the contact at which point the sliding velocity and its component in the squealing mode direction are determined. The friction behaviour and parameters are governed by the contact mechanics which transfer friction forces and couple with the dynamics of the dominant modes of vibration of the brake system. If the interaction is unstable, the resultant brake system vibrations grow into a squeal limit cycle

which in turn creates noise [18],[19]. The main aim of this paper is to investigate and quantify when the squeal limit cycle breaks up into chaotic motion. It is possible that this could occur under mode coupling, causing very large instability levels resulting in averaged localised phase space expansion [31]. In the following, the full nonlinear numerical and simplified analytical models used for this purpose are described.

2.1. Full Nonlinear Brake Squeal Model

The full nonlinear interactions of the brake system of Figure 1, can be encapsulated by the two dgree of freedom model of Figure 2 [18]. The derivation of the equations of motion are provided in [18], so for convenience are just summarised in the following. Figure 2 a) shows the total sliding velocity, V, at a brake pad angle of attack, θ_A, to the perpendicular components, V_o and crabbing velocity, V_c. The contact between the rotor and pad under static and dynamic normal force, N, F_N, induces a friction force, F_f, that couple the two dominant uncoupled spragging and out of plane modes, a, b, at a sprag angle, θ, shown in Figure 2(b).

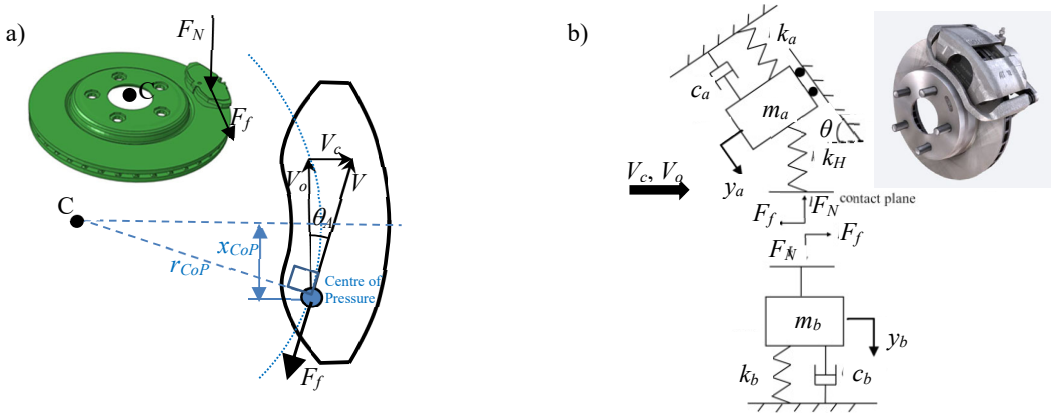

Figure 2 Two degree of freedom model for brake squeal consisting of; (a) brake pad mechanics with sliding and friction forces acting through the centre of pressure, and (b) coupled modal dynamics [18]. *Insets: Abaqus & Free3D Car Brake System models.*

According to Figure 2a), the quasistatic brake pad angle of attack, θ_A, is determined geometrically as,

$$\sin(\theta_A) = V_c/V = x_{CoP}/r_{CoP}, \tag{1}$$

where x_{CoP} and r_{CoP}, define the position of the Centre of Pressure. Alternatively, the dynamic sliding ratio which includes the vibration component in the contact plane is defined as,

$$\zeta = \left(V_{c,o} + (\delta_a \dot{y}_a(t)\, cos(\theta))\right)/V, \tag{2}$$

where δ_a is the sliding direction defined as +1 in Figure 2 b. The contact mechanics couples two dominant uncoupled modes at a sprag angle according to Figure 2b), as,

$$m_a\ddot{y}_a(t) + c_a\dot{y}_a(t) + k_a y_a(t) = -F_N\, sin(\theta) - F_f\, cos(\theta), \quad m_b\ddot{y}_b(t) + c_b\dot{y}_b(t) + k_b y_b(t) = F_N \tag{3}$$

$$\text{where} \quad F_N = k_H(y_a\, sin(\theta) - y_b), \quad F_f = \delta_a\, \mu(\zeta)(N + F_N), \tag{4}$$

where, y, m, k, and c are the uncoupled modal displacements, masses, stiffnesses, and damping coefficients, respectively. A smooth nonlinear friction law is used from [26] to represent both large and small vibrations as a function of the dynamic sliding ratio,

$$\mu(\zeta) = \mu_s\, tanh(\alpha_\mu \zeta)[\mu_k + (1 - \mu_k)\, sech(\beta_\mu \zeta)]. \tag{5}$$

where μ_s and μ_k represent the static and dynamic friction coefficients and α_μ and β_μ determine the shape of the friction curve. The friction curves of (5) are shown in the results as *Figure 3*, for a fundamental and real brake system that has been tuned to measurements in [24].

The equations (1)-(5), represent the full nonlinear equations of motion of the system that can be solved numerically. Analytical solutions for predicting the occurrence growth and amplitude of squeal limit cycles are described in the subsequent section 2.2.

2.2. Analytical solutions for brake squeal limit cycles

The local stability and growth of brake squeal can be determined using a complex eigenvalue analysis. This is typically performed numerically due to mathematical difficulties, however an analytical solution was recently obtained in [23] under the assumptions of small non-proportinal damping. In such a away, the coupled equations (3) and (4) can be decoupled to the form,

$$\mathbf{p_L}^{\mathbf{T}}\mathbf{M}\mathbf{p}\ddot{\mathbf{Y}} + \mathbf{p_L}^{\mathbf{T}}\mathbf{C}\mathbf{p}\dot{\mathbf{Y}} + \mathbf{p_L}^{\mathbf{T}}\mathbf{K}\mathbf{p}\mathbf{Y} = \mathbf{p_L}^{\mathbf{T}}\mathbf{F}, \qquad \boldsymbol{Y} = \mathbf{p}^{-1}[y_a \quad y_b]^T, \qquad \mathbf{F} = [-\delta_a\, \mu(\zeta) N\, cos(\theta) \quad 0]^T \tag{6}$$

where **Y** is the decoupled modal displacement vector and **M**, **K**, **C**, and **F** are the, mass, stiffness, damping matrices and forcing vector of equations (3) and (4), respectively. The left and right undamped eigenvectors $\mathbf{p_L}$ and **p,** are defined as,

$$\mathbf{p_L} = \begin{bmatrix} 1 & p_{L2} \\ p_{L1} & 1 \end{bmatrix} \text{ where } \mathbf{p_L}^{\mathbf{T}}\mathbf{K} = \lambda^2 \mathbf{p_L}^{\mathbf{T}}\mathbf{M}, \quad \mathbf{p} = \begin{bmatrix} 1 & p_2 \\ p_1 & 1 \end{bmatrix} \text{ where } \mathbf{K}\mathbf{p} = \lambda^2 \mathbf{M}\mathbf{p}. \tag{7}$$

where p_i and p_{Li} are the eigenvector elements that determine the eigenvalues and therefore the system modal damping as a function of system parameters, as [23],

$$p_1 = \left[{\omega_a}^2 - {\omega_b}^2 + \sqrt{\Delta}\right]/[2f(\mu,\theta)\, k_H/(m_a\, sin(\theta))],\ p_2 = 1/\bar{p}_1,\ p_{L1} = -m_a/\bar{p}_1 m_b,\ p_{L2} = -m_b/\bar{p}_2 m_a$$

$$\text{therefore} \quad p_L p_i = 4f(\mu,\theta)\left(k_H/m_j\right)^2/\left[{\omega_a}^2 - {\omega_b}^2 - \sqrt{\Delta}\right]^2, \quad \text{where} \quad f(\mu,\theta) = sin^2(\theta)(1 + \delta_a \mu/\, tan(\theta)),$$
$$ {\omega_a}^2 = (k_a + k_H f(\mu,\theta))/m_a,\ {\omega_b}^2 = (k_b + k_H)/m_b,\ \Delta = ({\omega_a}^2 - {\omega_b}^2)^2 + 4f(\mu,\theta){k_H}^2/(m_a m_b). \tag{8}$$

Here *i* is the mode number, *j=b,a*, $\bar{}$ is the conjugate, *f(μ,θ)* represents Spurr's [3] criteria for spragging $\tan(\theta) < -\delta_a \mu$ and Δ is the discriminant that determines whether the eigenmodes are real or complex and therefore the type of mode coupling (see [18] for more details). In particular, if Δ is positive, the eigenvalues are real and viscous mode coupling occurs (coupling determined by the damping matrix). Conversely, if Δ is negative, the eigenvalues are complex and stiffness mode coupling occurs (coupling determined by the stiffness matrix). The additional effect of falling friction on the stability is determined by the friction curve. For localised behaviour, the nonlinear friction law of (5) can be approximated as a curve with bilinear slopes, $k_{\mu 1}$ and $k_{\mu 2}$, as,

$$\mu(\zeta) = \begin{cases} k_{\mu 1}\zeta' & \text{for } \zeta' \le 1 \\ k_{\mu 1} + k_{\mu 2}(\zeta' - 1) & \text{for } \zeta' > 1 \end{cases} \quad \text{where} \quad \zeta \ge -\zeta_c \ \text{ and } \ \zeta' = \zeta/\zeta_c, \tag{9}$$

where, ζ_c, is the critical sliding ratio at the peak friction that is approximated to within 5% error as [18],

$$\zeta_c \approx W_0\left(8(\alpha_\mu/\beta_\mu)^2/(1-\mu_k)\right)/(2\alpha_\mu) \quad \text{if} \quad \beta_\mu/\alpha_\mu \le 0.25, \tag{10}$$

where $W_0()$ is the positive solution to the Lambert W function. The approximation (9) has been tuned to measured brake friction curves as shown later in *Figure 3*. The approximations (3), (6), (9) can be combined to provide analytical equations of motion for the decoupled modes *i = 1,2,* as,

$$m_i\ddot{y}_i(t) + c_{eff}\dot{y}_i(t) + k_i y_i(t) = 0, \text{ where } c_{eff} = c_{si} + k_{Fi}k_{\mu 1,2}N/(\zeta_c V),\ k_{F1} = 1,\ k_{F2} = p_{L2}p_2 \tag{11}$$

and c_{eff} is the effective system damping (including falling friction), $k_{\mu 1,2}$ is the local friction curve slope at sliding velocity $V_{o,c}$ and the coupled system modal parameters are,

$$m_i = \mathbf{p_L}^{\mathbf{T}}\mathbf{M}\mathbf{p}_{i,i},\ k_i = \mathbf{p_L}^{\mathbf{T}}\mathbf{K}\mathbf{p}_{i,i},\ c_i = \mathbf{p_L}^{\mathbf{T}}\mathbf{C}\mathbf{p}_{i,i} \tag{12}$$

and c_{si} represents the system modal damping of the coupled structure (without falling friction),

$$c_{si} = \begin{cases} c_i & \text{if } p_i, p_{Li} = Re(p_i), Re(p_{Li}) \\ Re\left(c_i/(2m_i) \pm \sqrt{{c_i}^2/(2m_i)^2 - k_i/m_i}\right) 2m_i & \text{if } p_i, p_{Li} \ne Re(p_i), Re(p_{Li}) \end{cases} \tag{13}$$

Equation (13) highlights that the system modal damping, c_{si}, depends on the complexity of the eigenmodes and therefore the type of mode coupling (ie viscous or stiffness). Since the structural modal damping factors are usually well below critical, it may be deduced from (13) that stiffness mode coupling (second line) provides a much larger contributioin to the system modal damping (and local eigenvalue magnitude) than viscous mode coupling (first line). The stability and hence occurrence of brake squeal can then be simply expressed according to when the effective system damping becomes negative and analytically determined using equations (11) and (13) as,

Instability / squeal when: $$c_{eff} = \left(\underline{c_{si}} + \underline{k_{Fi}k_{\mu 1,2}N/(\zeta_c V)}\right) < 0 \tag{14}$$

Structural damping (-ve if Spragging and Mode Coupling)

Friction slope damping (-ve if Falling Friction)

The brake squeal criterion (14) concisely combines and superposes the effects of mode coupling and falling friction via the effective system damping, $c_{eff.}$ Squeal instability will initially grow exponentially when the effective system damping, c_{eff}, is negative but this growth will change with amplitude as c_{eff}changes. In particular, when the sliding oscillation amplitude encroaches on the friction stick region below critical friction, positive damping will be added. At

a particular oscillation amplitude, $A_a\omega_i$, where the power from the negative damping exactly balances the positive damping ,a steady state limit cycle will occur according to [18][26],

$$A_a\omega_i = \left((V_{c,o} - \zeta_c V)/(cos(\theta)\, cos(\omega_i t_c)\right) \text{ where } sin(2\omega_i t_c) - 2\omega_i t_c = 2\pi\left(\zeta_c V c_{si}/(k_{Fi}N) + k_{\mu 2}\right)/\left(k_{\mu 1} - k_{\mu 2}\right) \tag{15}$$

where t_c is the time in the squeal cycle that the sliding ratio reaches the critical peak of the friction curve. The closed form solution of (15) assumes a linear sinusoidal limit cycle. This assumption may be broken under larger amplitude nonlinear phenomena such as chaotic motion [25],[26],[31]. Therefore, Equations (8), (11)-(15) provide closed form analytical solutions to brake squeal limit cycle occurrence, initial growth and amplitude under the instability mechanisms of mode coupling and falling friction.

2.3. Prediction of Brake Squeal Chaos

What happens when the squeal limit cycle breaks down due to excessive instability levels causing phase space expansion? In the following, two analytical criteria for the prediction of chaotic vibrations in brake squeal are developed based on the Lyapunov exponent (expansion) test for chaos and the analytical solutions developed in 2.2. The Lyapunov exponent test measures the sensitivity of the system to changes in initial conditions. In particular, the Lyapunov exponent, λ, defines the power law growth or expansion of the change in size of an initial error condition according to [34],

$$d = d_o 2^{\lambda(t - t_o)}\ , \tag{16}$$

where, d, is the maximum diameter of the ellipsoid in phase space that grows from the initial conditions at time t, and d_o is the diameter of the sphere of initial conditions at time t_o. A positive Lyapunov exponent implies chaos ie,

$$\text{chaos if} \qquad \lambda > 0. \tag{17}$$

In a chaotic system the motion is bounded by nonlinearities so its divergence, λ, is measured locally using small time increments $t - t_o$ or linearly using partial derivatives (the Jacobian matrix) and continual resetting to obtain an average local divergence over a long period of time. Similarly, the eigenvalues of the Jacobian matrix determine the local stability such that there is a close relationship between the maximum Lyapunov exponent and system eigenvalue evaluated dynamically, ie in a general case, the maximum Lyapunov exponent can be shown to be an average of the real part of the maximum dynamic eigenvalue integrated over a sufficiently long time period [35]. Therefore, chaos is most likely to occur when the largest eigenvalue is most positive, indicating the highest local divergence. In the present brake squeal case, the stability and eigenvalue analysis has been determined analytically in section 2.2. It is found that the largest eigenvalue is most positive when the effective system damping c_{eff} in the modal equation (11) is most negative. This occurs under stiffness mode coupling conditions in typical brake squeal conditions because the modal damping factor is less than critical, causing the complex stiffness to have a larger instability effect than the modal damping (13). Therefore, a simple, conservative analytical solution for the critical friction coefficient at which brake squeal chaos may occur may be obtained, based on the occurrence of stiffness mode coupling, as:

$$\text{Chaos if} \qquad \mu_s > \mu_{crit}, \quad \Delta(\mu_{crit}) = 0, \tag{18}$$

where a fully closed form analytical solution for the critical friction for chaos may be obtained using (8) and (18), as,

$$\mu_{crit} = \left\{\frac{m_a}{k_H}\left[2\sqrt{\frac{k_H}{m_b}\left(\frac{k_a}{m_a} - \frac{k_b}{m_b}\right)} - \left(\frac{k_H}{m_b} + \frac{k_a}{m_a} - \frac{k_b}{m_b}\right)\right] - \sin^2(\theta)\right\}/(\delta_a\, cos(\theta)\, sin(\theta)). \tag{19}$$

Equations (18) and (19) represent a conservative criterion for brake squeal chaos in that only the condition for high local phase space expansion due to stiffness mode coupling is considered. As it is based on the largest eigenvalue of the system it has not taken into account the continuous averaging of the local expansion at many points around the phase space. Also bounded chaos requires sufficient nonlinearities for folding and contraction in the phase space. This may be taken into account by also defining an amplitude criterion at which substantial expansion and nonlinearities occur.

For this purpose, the closed form limit cycle solution for brake squeal **(15)** may be used to solve for when the bilinear friction law **(9)** is exceeded causing large nonlinearities associated with negative creep oscillations [31]. Therefore the critical condition for the possible breakup of the limit cycle to nonintegrable behavior may be defined by the necessary condition,

$$A_a\omega_i \geq V_{c,o}/\cos(\theta) \quad \text{for } V_c > \zeta_c V_o\,. \tag{20}$$

This conservative condition may be simplified by solving for the critical system modal damping using (20) and the solution **(15)**, as,

$$\text{Chaos if } \mu_s > \mu_{crit},\ c_{si}(\mu_{crit}) = k_{Fi}N\left[\left((sin(2\omega_i t_c) - 2\omega_i t_c)\left(k_{\mu 1} - k_{\mu 2}(\mu_{crit})\right)/2\pi\right) - k_{\mu 2}(\mu_{crit})\right]/(\zeta_c V), \quad \omega_i t_c = acos(1 - \zeta_c V/V_c) \tag{21}$$

Equation (21) represents a less conservative criterion for brake squeal chaos than (18) and (19), ie in addition to large local expansion it assumes negative sliding is required to provide sufficient nonlinearities, to bound the brake squeal phase space behavior. In this case, the analytical solution is not fully closed form, so a numerical root finding function is required to find the solution for μ_{crit} from the analytical equations for c_{si} in (8),(11)-(13). However, in practice, this

computational time was found to be almost instantaneous. Note that the effect of parametric excitation due to changing friction levels [31] has been neglected due to the very steep positive slope of the friction curve and to avoid multiple lengthy integrations. This assumption is tested in the next section. In particular, comparisons of numerical solutions of the full nonlinear equations of motion are compared with these conservative predictive criteria for brake squeal chaotic instability ((18)&(19) and (21)) subsequently in section 3.

3. Results

The occurence of chaotic instability in brake squeal was investigated for two case studies [18] using the full nonlinear time domain model, described in section 2.1. The numerical solution of the full nonlinear equations of motion in section 2.1 were solved on an INTEL Core i7 using the fourth and fifth order Runge–Kutta routine using DYNAMICS by Nusse and Yorke, or the Radua method in MathCad 15.0 and an initial velocity at or smaller than 0.01 m/s. The time step was set at least 100 times smaller than the sprag mode natural period of oscillation, $2\pi/\sqrt{(k_a/m_a)}$. The nonlinear phenomena was investigated using various phase space tools and the Lyapunov spectrum of exponents using Wolf et al. [42] and iterated at least 1000 squeal oscillation periods. Comparisons of the full numerical solutions and the conservative analytical criteria derived in section 2.3 were performed and used to identify conditions under which chaotic instability occurs and its suppression over a range of friction coefficients, modal damping constants, sprag angles and brake pressures. The system nominal parameter conditions were chosen according to fundamental and real investigations of brake squeal, [21], [28], [15], [18] and [24] as described in Table 1.

Table. 1 *System parameters for fundamental and real brake squeal conditions.*

Description	**Fundamental Model** [21],[28], [18]	**Real Brake system Model** [15]
Structural vibration parameters		
Modal mass: (m_a, m_b)	1, 0.866 kg	2.716, 9.815(@10psi) kg
Modal stiffness: (k_a, k_b)	17.93, 2.656 N/m	9.078E8, 2.442E9(@10psi) N/m
Modal damping: (c_a, c_b)	0.3, 0.26 Ns/m	3.6E3, 1.3E4 Ns/m
Contact stiffness (k_H)	20 N/m	1.131E9(@10psi) N/m
Sprag angle: (θ)	21.14º	17.35º
Friction curve parameters [24]		
Static friction coefficient constant (μ_s)	0.5	0.8
Critical sliding ratio (ζ_c)	0.021	0.00748
Stick slope ($k_{\mu 1}$) – analytical model	0.5	0.8
Sliding slope ($k_{\mu 2}$) – analytical model	-5.62E-5 (@1.047 m/s,μ_s=0.5)	-1.0E-4 (@0.628 m/s,μ_s=0.8)
Friction curve parameter (α_μ) – simulation model	300	1000
Friction curve parameter (β_μ) – simulation model	1	1
Kinetic friction ratio (of static friction) (μ_k) – simulation model	0.83	0.83
Squeal nominal conditions		
Nominal brake pad angle of attack (θ_A)	0 rad	100 mrad
Nominal normal loading (N)	40 N	100 N
Nominal sliding velocity (V)	1.047 m/s	0.628 m/s
Initial sprag mode velocity	0.01 m/s	0.001 m/s
Notes: ($@\mu$=0.5) indicates this parameter value is a function of friction coefficient and was evaluated at this nominal value. ($@$10psi) indicates this parameter value is a function of brake pressure and was evaluated at this nominal value.		

The nonlinear friction model of equation (5) was tuned experimentally to a typical automobile pad (Volvo 850/S70 X8 pad) [24]. Note that lower friction curve steepness parameters, α_μ, to [18] were used to provide the same accuracy of fit while enhancing the numerical stability and speed of the solver. The approximate bilinear friction curve parameters $k_{\mu 1}$ and $k_{\mu 2}$ were obtained automatically from the experimentally tuned nonlinear friction model according to [26],

$$k_{\mu 1} \approx \mu(\zeta_c) \text{ and } k_{\mu 2} \approx (\mu(2\theta_A) - \mu_s)\zeta_c/(2\theta_A). \quad (22)$$

These experimentally tuned nonlinear and approximate bilinear friction curves of equation (5) and (22) were plotted over a large sliding velocity range in Figure 3.

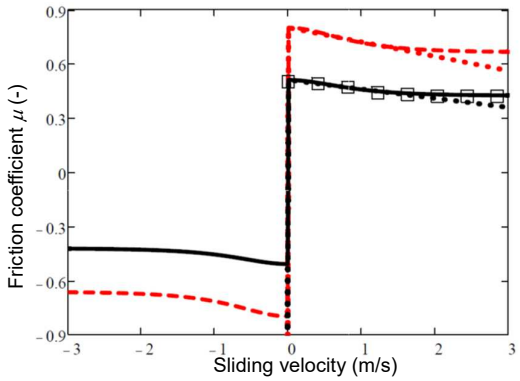

Figure 3 *The friction curve for μ_s=0.5; simulated using equation* (5); fundamental and real brake system models *(-),(- -), analytical bilinear approximation at 1m/s (..),(..) and experimentally measured (averaged) for Volvo 850/S70 X8 pad(□)[24].*

The curves of Figure 3 show the experimental friction curve including falling friction can be well represented by the full nonlinear curve (5) and the analytical bilinear approximation with less than 2% and 5% error, respectively, for the fundamental model. The nominal higher static friction level of the real brake system model is also represented reasonably with the falling friction notably having a higher slope according to (5) and (22). These friction models are used to investigate the onset and control of chatic instability in brake squeal in the following.

3.1. Numerical Identification of Brake Squeal Chaos in a Fundamental System.

A fundamental degree of freedom brake squeal model [21],[28],[18] was investigated for nonlinear squeal instability as the friction coefficient was changed. The fundamental model parameters were chosen as described in [18] and are listed in the first column of *Table. 1*. The local stability of the equations of motion using (13) were verified with full numerical complex eigenvalue solutions in [18] for varying friction coefficient. It showed two mode solutions with distinct frequencies up to a critical value of $\mu = 0.453$. Beyond this, stiffness mode coupling occurs where the modes have the same natural frequency but opposing complex stiffness damping levels that are increased by the structural modal damping. The complex stiffness negative damping increases as the friction coefficient increases further until it is balanced by the positive structural damping at $\mu = 0.47$ at which point a squeal limit cycle occurs. This transition to a limit cycle as the friction increases represents a Hopf bifurcation. The amplitude of the limit cycle is determined by the nonlinear friction curve which may introduce nonlinear instability ie chaotic motion.

To investigate the nonlinear behaviour, time histories and phase spaces of numerical solutions of the nonlinear differential equations of motion, were first determined under the static friction levels, μ_s, of 0.65 and 0.85 as shown in *Figure. 4*.

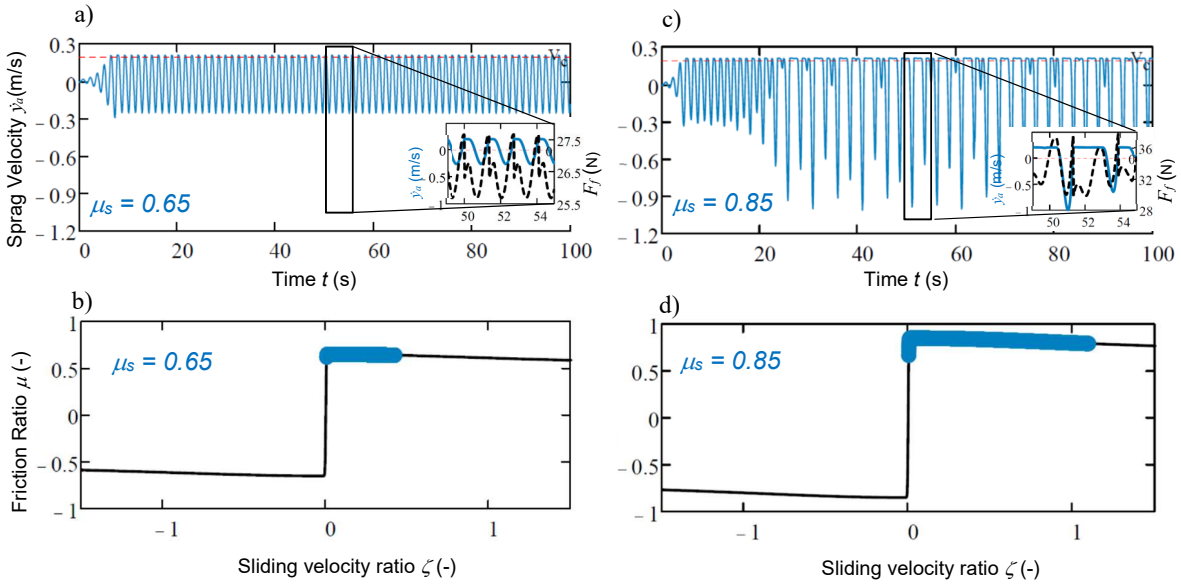

Figure. 4 *Simulated squeal oscillations for fundamental brake system; a) sprag mode vibration velocity (-) and b) corresponding friction oscillation range (━) under static friction μ_s=0.65 and c) sprag mode vibration velocity (-) and d) corresponding friction oscillation range (━) under static friction μ_s=0.*

The time history of *Figure. 4* a) shows that brake squeal occurs after a small period (~7s) of exponential growth to reach a constant limit cycle amplitude for a static friction level, μ_s=0.65, exceeding the critical Hopf bifurcation value. The oscillations are approximately sinusoidal as predicted by the local stability analysis. The corresponding friction oscillations shown in *Figure. 4* b) are mainly on the negatively sloped region of the friction curve, encroaching only a very small part of the steep positively sloped region to provide the necessary power dissipation to achieve the limit cycle energy balance. In contrast, when the static friction is increased to μ_s=0.85, *Figure. 4* c) shows much larger, irregular, non-sinusoidal, sprag velocity oscillations. Similarly, comparison of the cases of *Figure. 4* b) and d) highlight much larger friction oscillations with larger encroachment on both the positive and negative slopes. Note that in this case, although it is approaching negative (or reverse) friction as the static friction is increased, the large irregular squeal oscillations have not encroached into this negative sliding state which is in contrast with the predictions of chaotic motion for an analogous wheel squeal case [31]. This should be investigated further as it appears the nonlinear effects associated with the chaotic motion are due to the friction curve shape over the positive stick and sliding region alone (see *Figure. 4* d). This is found in the forced one degree of freedom friction oscillator system of [26] but in contrast to the positive and negative sliding behaviour found in [31]. Based on the damping magnitudes from the system structural damping (c_{si}=-0.11 Ns/m) and positive and negative sloped sticked region ($k_{Fi}k_{\mu 1,2}N/(\zeta_c V)$= 1532 and -0.99 Ns/m, respectively) it would appear that there is a sudden change in damping force at critical sliding that in this case is distorting the sliding velocity from a linear sinusoidal shape. This would tend to suggest that the chaotic behaviour is due to the bilinear nature (with one slope approaching infinity) of the friction curve (not trilinear) as consistent with [26][32][33]. In particular, the large non-sinusoidal oscillations for the case *Figure. 4* c) and d) indicate linear assumptions of the predictive limit cycle analysis (9) and (15) are invalidated. To investigate this possible chaotic instability in more detail, further numerical nonlinear analyses were performed in the following.

The onset of brake squeal chaos in the phase space was investigated under increasing static friction coefficient as shown in *Figure. 5*.

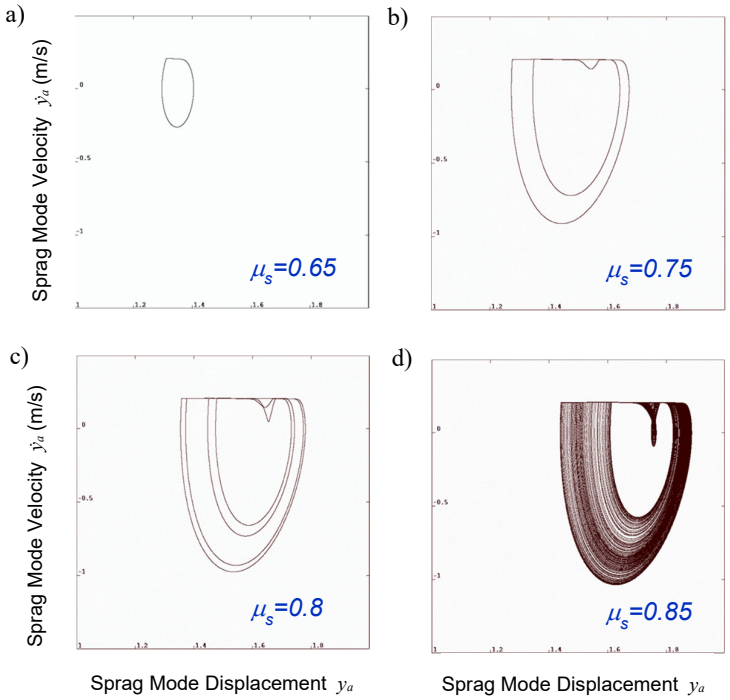

Figure. 5 Phase spaces of brake squeal oscillations under increasing static friction coefficient; a) μ_s=0.65 b) μ_s =0.75 c) μ_s =0.8 and d) μ_s =0.85.

Figure. 5 depicts brake squeal behavior changing from a one-loop limit cycle and bifurcating to more complex nonlinear behavior. In particular, *Figure. 5* a) shows a small closed single loop limit cycle for μ_s =0.65 indicating approximately sinusoidal squeal behavior. For initial conditions further away from this smaller loop, a different larger limit cycle was found similar to the inner loop of *Figure. 5* b). As the static friction coefficient is increased to μ_s =0.75 (*Figure. 5* b) the limit cycle bifurcates into two-loop motion that bifurcates again as the contact angle is increased to μ_s =0.8. Further increases in static friction to μ_s =0.85 caused further increasingly compressed bifurcations to a wandering orbit that appears to not be closed. This could indicate chaotic instability. For confirmation, the corresponding Poincare maps and bifurcation diagram were calculated as all shown in *Figure. 6*. The Poincare plane of y_b=0.6 was chosen for convenience.

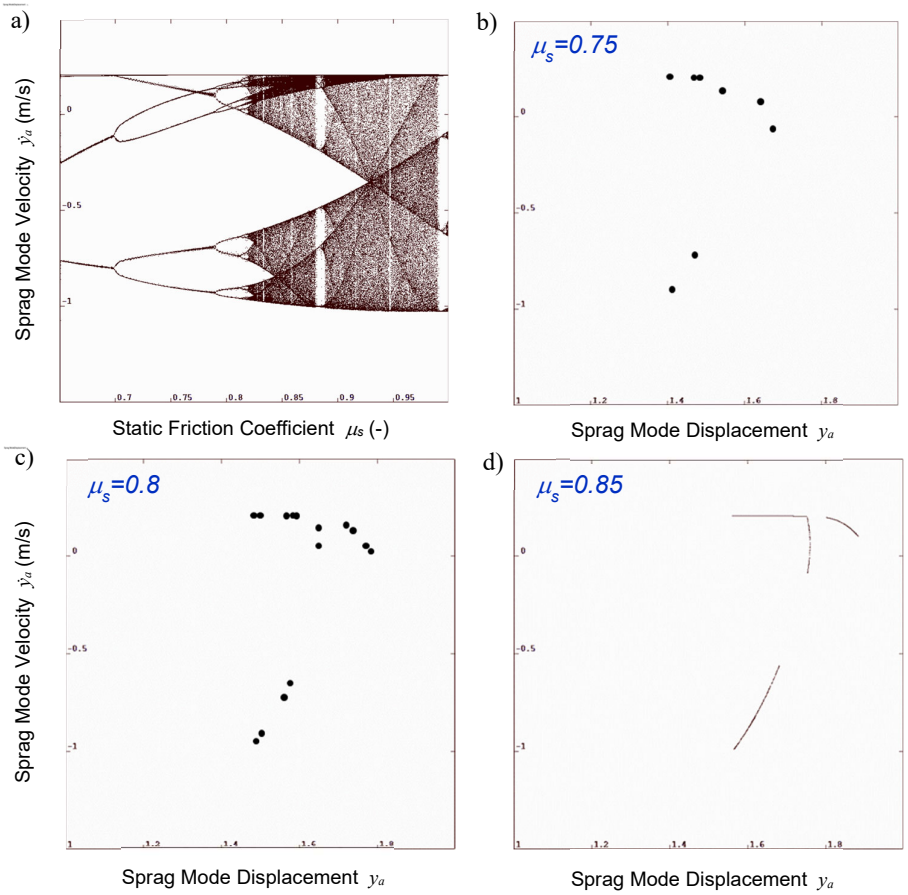

Figure. 6 a) Bifurcation diagram of Poincare maps for static friction coefficient. Poincare maps for increasing static friction coefficients; b) μ_s =0.75 c) μ_s =0.8 and d) μ_s =0.85.

The nonlinear behavior of the phase spaces of *Figure. 5* appear to be confirmed in *Figure. 6*. In particular, the bifurcation diagram of *Figure. 6*a) shows a period 4 limit cycle, at low static friction coefficient, bifurcating via a well-known period doubling route to chaos as friction increases. The two-loop phase space behaviour of *Figure. 5* b) at μ_s =0.75 is confirmed by the Poincare map of *Figure. 6* b) with a closed set of 8 points indicating period 8 limit cycle behaviour. The bifurcation diagram of *Figure. 6* a) shows a branching to period 16 limit cycle in *Figure. 6* c) and further increasingly compressed bifurcations to the onset of chaos at $\mu_s > 0.82$. This is shown in the Poincare map of *Figure. 6* d) as an approximate one dimensional fractal, characterised by the nonperiodic random like behavior in the phase space of *Figure. 5* d). This strange attractor was determined to have a Lyapunov Dimension of 2.85 with the fractal nature confirmed by the non-integer value. This was calculated using the Lyapunov spectrum of [0.142 0.0 -0.167 -454] with the positive maximal exponent confirming chaotic instability via exponential sensitivity to initial conditions. Note that for a static friction coefficient of μ_s =0.883 there occurs a window of periodic behavior with a closed set of approximately 12 points (with evidence of some overlapping in *Figure. 6* a). This typical period doubling route to chaos in brake squeal is in contrast to the quasiperiodic route found for wheel squeal in [31] but is consistent with the forced friction oscillator chaos with the same fricton model in [26]. Interestingly, it is noted that in this case, chaotic instability occurs without a nonlinear jump to brake squeal negative sliding amplitudes. This is inconsistent with [31] but encapsulated by the first conservative criteria developed in section 2.3. This identification and onset of brake squeal chaos was investigated further in a real brake system.

3.2. Numerical identification of brake squeal chaos in a real brake system.

A similar nonlinear investigation to section 3.1 using the two degree of freedom brake squeal model (2.1) was performed on a real brake system with coupled in and out of plane modes that was experimentally verified in [15]. The analytical and numerical predictions of the occurrence and growth of limit cycle squeal are provided in [18] and are verified by a comprehensive set of brake squeal experiments detailed in [15]. In particular, the measured braking conditions under which brake squeal occurred on the floating caliper brake assembly were verified with the theoretical modelling but chaotic phenomena were not investigated. The squeal mode was measured to have a frequency of 3kHz [15] and found to correspond to finite element model results in *Figure 7* a) [18] .

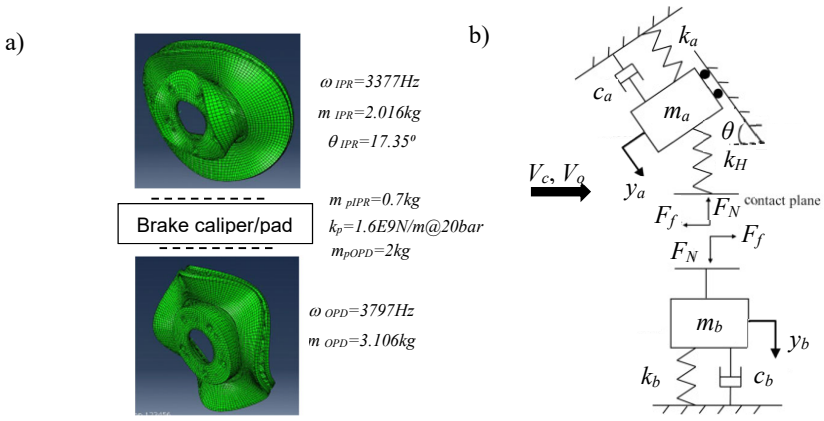

Figure 7 Real brake system squeal model (a) coupled in-plane radial (IPR) and out of plane diametral (OPD) modes [15], [18] (b) coupled two mode brake squeal model [18].

Dynamic transformations of *Figure 7* a) where used to determine the parameters listed in *Table. 1* for modes *a* and *b* in Figure 7*b)*, based on the coupled rotor and brake calliper dynamics, as detailed in [18]. One of the key characteristics of real brake squeal is its dependence on brake pressure [15]. This is most likely due to contact stiffness variation from loading of rough elastic surfaces and non-elastic behaviour, that may be modelled as [18], [29],

$$k_H(p) = k_{Ho} p^{1/2}, \tag{29}$$

where p and k_{Ho} are the brake pressure and a proportional factor tuned to the nominal conditions, respectively. In this case, the brake pressure exponential coefficient of ½ is chosen for a typical contact roughness fractal distribution according to [30]. Hence, the contact stiffness and modal stiffness and mass parameters, b, are functions of pressure p as detailed in [18]. In the following cases, when the damping was changed from the nominal damping ratios of 3.6% and 4.2% for the *a* and *b* modes, respectively, the scaling $c_b=3.613\ c_a$ was preserved. To investigate the nonlinear behaviour in this real brake system, numerical simulations of the time history and friction curve behaviour, were first investigated under nominal and greatly reduced (10%) damping levels as shown in *Figure. 8*.

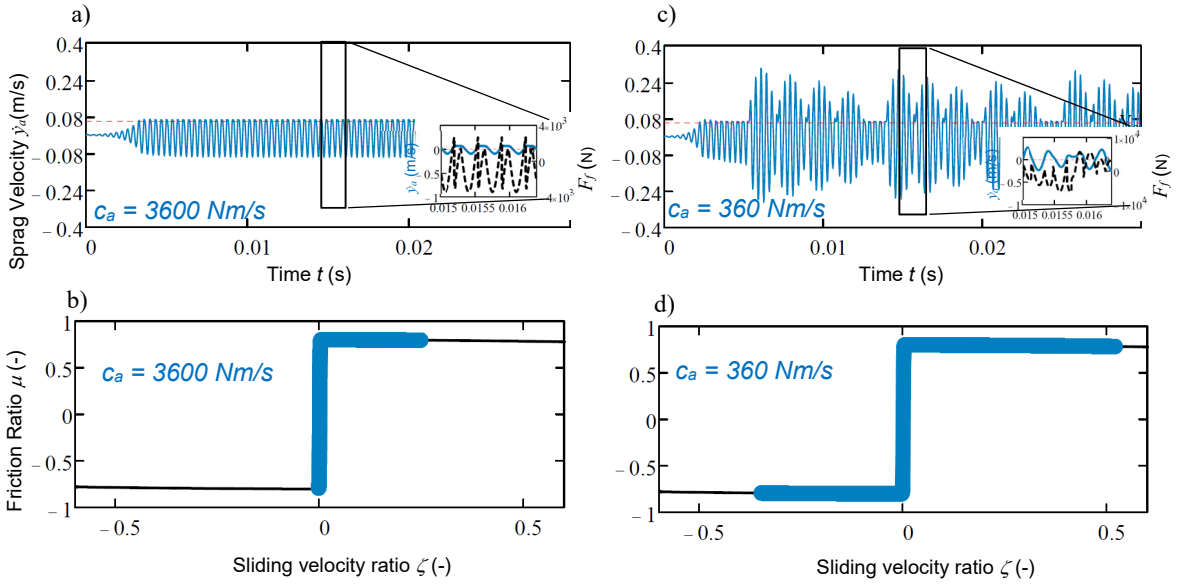

Figure. 8 *Simulated squeal oscillations for real brake system; a) sprag mode vibration velocity (-) and b) corresponding friction oscillation range (━) under static friction c_a=3600 Ns/m and c) sprag mode vibration velocity (-) and d) corresponding friction oscillation range (━) under static friction c_a=360 Ns/m. In all cases $c_b=3.613\ c_a$*

Similar to *Figure. 4*, *Figure. 8* shows brake squeal due to; a) a periodic limit cycle due to stiffness mode coupling and, c) a larger irregular amplitude time history for a much lower modal damping (10%). The corresponding friction oscillations shown in *Figure. 8* b) and d) highlight the low damping case has very large, positive and negative sliding which is not sinusoidal. In particular, comparing the time histories of *Figure. 8* a) and c), in the period up to 0.05s, it may be deduced that the oscillations grew to a nonlinear irregular amplitude once it encroached into negative (or reverse) sliding, as consistent with [31], but in contrast to *Figure. 4*. The very large irregular oscillations for the low damping case in the zoomup of *Figure. 8* c) and the sliding oscillations in *Figure. 8* d) indicate linear limit cycle assumptions of equations (9) and (15) are invalidated. In the following, further phase space and Poincare map investigations were performed.

A more detailed investigation of the onset of chaotic brake squeal under progressively lower damping is shown in the phase spaces of *Figure. 9*.

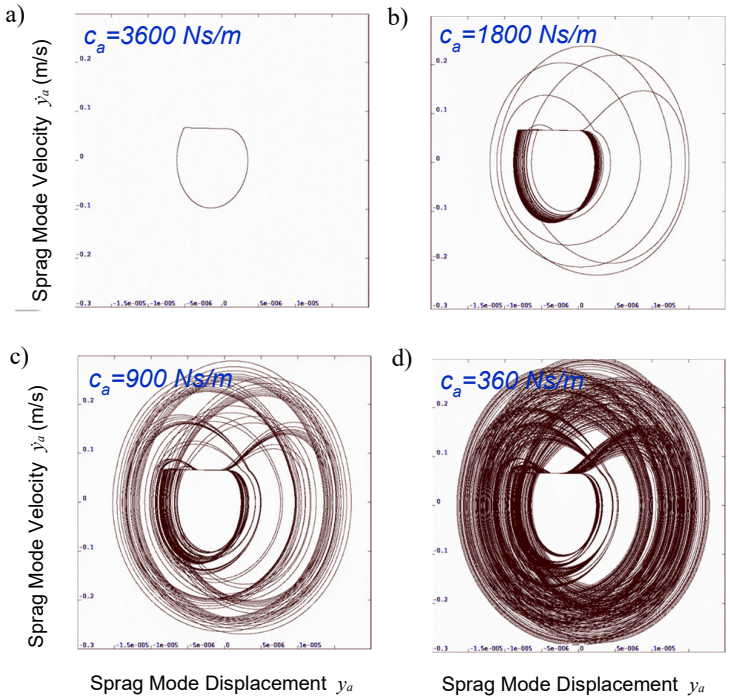

Figure. 9 Simulated phase spaces of squeal oscillations in a real brake system under decreasing damping; a) c_a=3600 Ns/m b) c_a=1800 Ns/m c) c_a=900 Ns/m and d) c_a=360 Ns/m. In all cases c_b=3.613 c_a.

Figure. 9 shows that the brake squeal behavior changes from a one-loop limit cycle and breaks into more complex possibly chaotic behavior. In particular, *Figure. 9* a) shows a simple closed limit cycle for c_a=3600 Ns/m indicating sinusoidal-like squeal behavior. As the damping was decreased to 50% nominal, shown in b), the limit cycle breaks into complex periodic motion that complicates further as the damping is decreased to 25% nominal damping. Further decreases in damping to 10% nominal damping leads to a wandering orbit that appears to not be closed. For confirmation, the corresponding bifurcation diagram and Poincare maps are shown in *Figure. 10*. The Poincare plane of y_b=0.0 was chosen for convenience.

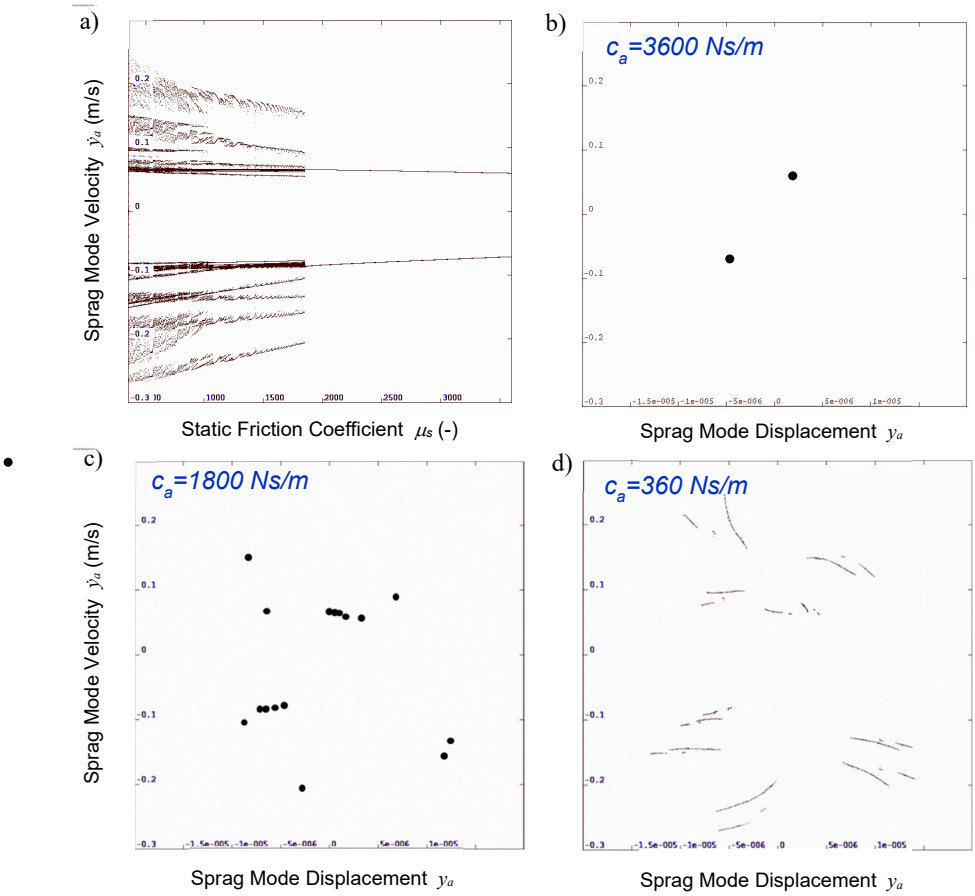

Figure. 10 a) Bifurcation diagram of Poincare maps for increasing damping in real brake system. Poincare maps for decreasing damping; b) c_a=3600 Ns/m c) c_a=1800 Ns/m and d) c_a=360 Ns/m. In all cases c_b=3.613 c_a.

Figure. 10 confirms the nonlinear behavior shown in the phase spaces of *Figure. 9* is brake squeal chaos. The bifurcation diagram (*Figure. 9*a) shows chaotic behaviour at the lowest damping levels of 10% nominal, that gradually becomes more ordered as the damping is increased. In particular, the sinusoidal squeal with single loop phase space at nominal damping of *Figure. 9*a) is confirmed to be period 2 motion in the Poincare map of *Figure. 10* b). The breakdown to complex periodic motion occuring around 50% nominal damping in *Figure. 9*b) is shown to be approximately a period 16 limit cycle in *Figure. 10* b). This breakdown appears to be through a sudden crisis phenomenon rather than period doubling bifurcations as shown in the bifurcation diagram of *Figure. 10*a). The bifurcation diagram shows further slurring of the Poincare map periodic points as the damping reduces to 10% nominal to obtain an approximate one dimensional fractal in the Poincare map of *Figure. 10* d) characterised by the nonperiodic random like behavior in the phase space of *Figure. 9* d). Brake squeal chaos is confirmed by a positive maximal exponent of the Lyapunov spectrum [71 0.0 -1062 -1.61x10^5]. The fractal nature of the strange attractor was confirmed with a non-integer of 2.07 for the Lyapunov Dimension based on the Lyapunov spectrum. One of the key observations of the these fundamental and real brake squeal cases is that chaotic motion occurs with and without a nonlinear jump to negative sliding oscillations. It is interesting to see if these contrasting cases can both be predicting using the necessary analytical criteria developed in section 2.3.

3.3. Comparison of Predictions of Brake Squeal Chaos.

The onset of steady state brake squeal chaos over a range of parameters was numerically and analytically investigated. The occurrence of a non-closed limit cycle was detected using the phase space and Poincare map analyses of figures 9 and 10 to determine the critical friction coefficient for a range of contact angles and brake pressures. These numerical solutions were then quantitatively compared with the sufficient analytical predictions of chaotic instability using Eqs. (18)-(21). For the fundamental brake model conditions, two cases with different chaotic behaviour were compared; the first being parameters studied in table 1 and the second where the damping and normal force was dropped to 30% and 0.8% of the nominal values, respectively. For the real brake model, the brake pressure was varied with the damping held at 10% of the nominal values of table 1 under which chaotic vibrations occurred as shown in Figures 9 and 10 d). ***Figure. 11*** summarises these results and highlights the conservative nature of the analytical prediction for the onset of steady-state brake squeal chaos.

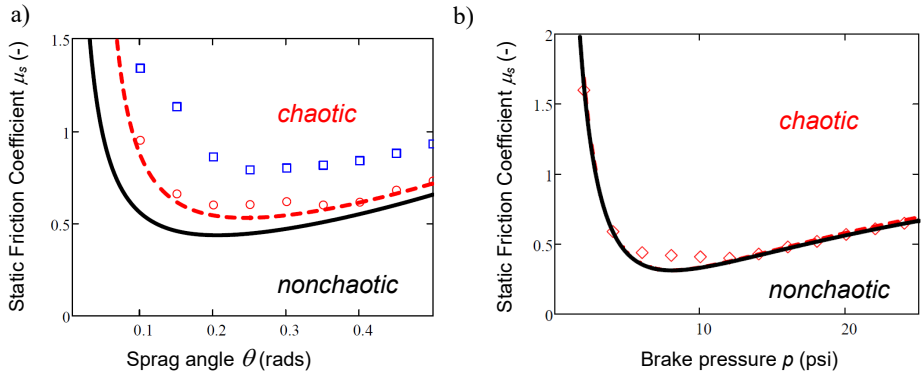

Figure. 11 a) Fundamental model, critical static friction coefficient vs sprag angle at which chaos first occurs;conservative analytical criteria; stiffness mode coupling (-), negative sliding (- -) and numerically simulated results for nominal conditions (□) and 30% and 0.8% nominal damping and normal force (o). b) Real brake model, critical static friction coefficient at which chaos first occurs conservative analytical criteria; stiffness mode coupling (-), negative sliding (mainly overlapping) (- -) and numerical simulations (◊) 10% nominal damping.

The fundamental model behavior of ***Figure. 11***. a) shows a good comparison between the analytically predicted onset of chaotic instability at critical static friction coefficient levels and that from the full nonlinear numerical simulations. In particular, the onset of chaos over the range of sprag angles is conservatively predicted by the negative sliding criterion to within 15% errors for the first case with lower damping, and normal force (o). A very similar trend is also predicted by the more conservative, but simpler, stiffness mode coupling criterion with larger errors for this case. For the nominal case (□), the negative sliding criterion does not exist as the normal load is too large to reach negative sliding under those parameters. This was confirmed by the friction oscillation ranges in Figure 4 d). In this case, it appears chaos is occurring due to different nonlinearities in the friction curve, and therefore the negative sliding criterion does not apply. This could be investigated further. Conversely, the stiffness mode coupling criteria is still relevant and provides a useful conservative prediction of the initial occurence of chaos, with notably the trend of critical static friction coefficient vs sprag angle predicted well. Chaotic squeal is characterized by high static friction coefficient over 0.6 for a range of sprag angles causing stiffness mode coupling squeal.

The real model behavior of ***Figure. 11***. b) shows a well-matched comparison, of critical static friction levels, between the conservative analytical predictions and the numerical simulations for the onset of chaotic instability over a range of brake pressures with errors less than 25%. In particular, the onset of chaos over the range of brake pressures is also well predicted by both stiffness mode coupling and negative sliding criteria (18)-(21) which are almost overlapping each other. This closeness may be due to the very high sensitivity of brake squeal amplitude with static friction coefficient near to stiffness mode coupling conditions. This indicates that brake squeal chaos is firstly determined by the onset of stiffness mode coupling and secondly large nonlinearities in the friction curve due to negative sliding. Suppression of chaotic instability can therefore be achieved using the quantitative understanding of the parameters and their effect on verified criteria demonstrated in Figure 11.

3.4. Suppression of Chaotic Instability in Brake Squeal.

The suppression of the onset of chaotic instability in the real brake squeal model was explored further in Table 2 with the nominal damping at 10% of the values of table 1. In particular, the % change in nominal parameter value required to avoid chaotic instability by ensuring the critical static friction coefficient exceeds realistic values of $\mu_{crit} > 1$, was determined, using the verified analytical criterion for negative sliding. Note, in this suppression investigation, the friction sliding slope, $k_{\mu 2}$, is held constant as the friction coefficient changes to isolate its effects.

Table 2 Parameter change required to suppress brake squeal instability to excessive friction levels, $\mu_{crit} > 1$

Parameter Description		Change required for elimination ($\mu_{crit} > 1$)	Example practical suppression method (Control/Change in)
Structural vibration parameters			
Modal mass (for sprag angle, θ constant)	(m_a, m_b)	-62% or +29%,-23% or +166%	Rotor / calliper structural design
Modal stiffness (for sprag angle, θ constant)	(k_a, k_b)	-24% or +88%, +31%	Rotor / calliper structural design
Modal damping (for sprag angle, θ constant)	(c_a, c_b)	+6000%, +7160%	Structural / material / shim damping
Contact stiffness (for sprag angle, θ constant)	(k_H)	-77% or +2300%	Material / geometry / surface roughness
Brake pressure	(p)	-72% or +346%	Braking functional requirement
Sprag angle	(θ)	-98% or +158%	Structural geometry / dynamic parameter

Friction parameters		
Critical sliding ratio (ζ_c)	Not Possible	-
Sliding slope ($k_{\mu 2}$)	-789700%	Pad Material/friction modifier
Brake pad angle of attack (θ_A)	-95%	Structural geometry / pad end condition
Nominal sliding velocity (for angle of attack, θ_A constant) (V)	-99%	Braking functional requirement (difficult)
Normal loading (N)	+6100%	-

Table 2 highlights multiple means of eliminating chaotic instability in brake squeal by parameter control. In general, the results appear to reflect that chaotic instability is dependent upon the stiffness mode coupling occurrence that in turn is dependent upon how close the uncoupled mode frequencies are. In particular, the following observations from the results of Table 2 can be made:

- Brake squeal chaos can be suppressed by small changes in modal mass or stiffness (>±31%) by greatly reducing the squeal growth rate due to stiffness mode coupling. These results are similar to means of avoiding brake squeal entirely as found in [18].
- Very large changes in modal damping are needed (>+73x) to overide the negative damping due to the very high complex stiffness from stiffness mode coupling.
- Large changes in contact stiffness are required (>-77%) to eliminate chaos as it has a less direct effect of detuning the modes to lessen stiffness mode coupling.
- Brake pressure has a stronger effect than contact stiffness as it effects this and the sprag modal properties. As the brake pressure necessarily changes as the brakes are applied over a full range, it is difficult to avoid chaos by controlling this parameter.
- Brake squeal can be eliminated by avoiding the sprag condition for mode coupling [18] by large increases (>+158%) or decreases (<-98%) in the sprag angle, θ. The sprag angle is determined by the mode shapes and brake structural geometry.

Brake squeal chaos suppression via friction parameter control is generally harder to achieve according to:

- Brake squeal chaos can not be eliminated by controlling the critical sliding ratio (at maximum friction) because the falling friction mechanism is secondary in this case compared to stiffness mode coupling.
- An extremely large increase in magnitude (>7898x) and change in sign of the sliding slope is required for falling friction to dampen the negative damping from stiffness mode coupling. In his case, this change is not realistic due to the very high complex stiffness.
- Chaotic instability can be avoided by large decreases in sliding velocity, V, or brake pad angle of attack, θ_A, to reduce squeal amplitudes by moving the initial sliding oscillations closer to the positive damped stick region [27].
- Very large increases (>62x) in normal loading are required to avoid brake squeal chaos, in this case, although normal loading may effect the stability characteristics in a away not modelled by the criteria.

These results show the conservative analytical criteria can very efficiently evaluate and quantify several brake squeal chaos suppression techniques, without the need for lengthy and extensive multiple numerical integrations of the nonlinear equations of motion.

4. Conclusion

Brake squeal chaos, under 'falling friction' and mode coupling mechanisms, has been efficiently predicted and suppressed based on a two degree of freedom coupled model. Numerical solutions of the full nonlinear equations of motion show brake squeal chaotic instability was characterised by a period doubling route in a fundamental brake squeal model as the static friction coefficient was increased. A similar, analysis for a real brake system model also shows a less clear bifurcation process (via maybe crises) to chaotic instability as the modal damping is decreased. Mode coupling instability is shown to provide the necessary (phase space) expansion (or positive Lyapunov Exponent) for chaos via friction which first causes limit cycle behaviour via a Hopf bifurcation. This limit cycle is shown to break up into chaotic motion characterised by a Poincare map with an approximate one-dimensional attractor, similar to that found in a forced dry friction oscillator [26]. For the first time, conservative analytical criteria for brake squeal chaos are derived and numerically verified over a range of static friction coefficients, structural damping, sprag angles and brake pressures for both the fundamental and real brake models. The predictive criteria are based on high local phase space expansion due to the occurrence of stiffness mode coupling and very large squeal instability causing negative sliding nonlinearities. The analytical criteria are found to conservatively predict the critical friction levels over a range of sprag angles and brake pressures to within 25% error and are noted to be calculated almost instantaneously. Interestingly a fundamental model case of chaotic instability without negative sliding squeal oscillations is identified under mode coupling. This case is also conservatively predicted by the first criterion but further research is required to understand and predict its occurrence

more accurately. Further insight may be gained from the forced bilinear model of [32] which showed chaos when one slope tends to infinity (like the stick slope of the friction curve in the present model). Despite this, the results provide important predictive insight into conditions under which brake squeal chaos occurs and its suppression. In particular, the efficient criteria are used to perform a parametric control investigation to suppress brake squeal chaos by increasing the critical static friction level at which chaos occurs to above 1. The results show small changes in modal mass or stiffness ($>\pm 31\%$) can suppress chaos by greatly reducing the squeal growth rate due to stiffness mode coupling (due to closeness of the uncoupled modal frequencies). The brake pressure and sprag angle are shown to be important control parameters for avoiding chaos in brake squeal. Physically the sprag angle could be controlled via the structural dynamic parameters and the geometry of the brake system. Very large increases in modal damping ($>+73x$) are needed to override the negative damping from the local phase space expansion due to stiffness mode coupling. The falling friction mechanism is shown to be secondary in this case (by approximately 7900x) compared to stiffness mode coupling. The results could be verified experimentally but provide predictive insight into conditions under which brake squeal chaos occurs and its suppression. It is hoped that the analytical results for this generalised model may provide predictive insight into other types of friction induced chaotic instability.

Acknowledgments
The author acknowledges the generous editing provided by Andrew Leslie.

Declarations

Funding (information that explains whether and by whom the research was supported)
Not applicable.

Conflicts of interest/Competing interests (include appropriate disclosures)
The authors declare that they have no conflict of interest.

Availability of data and material (data transparency)
All required data is available in the manuscript or as referenced.

Code availability (software application or custom code)
Not applicable.

References

[1] J. Fieldhouse, N. Ashraf, C. Talbot, “The Measurement and Analysis of the Disc/Pad Interface Dynamic Centre of Pressure and its Influence on Brake Noise”, SAE Technical Paper 2008-01-0826.

[2] N.M. Kinkaid, O.M., O'Reilly, and P. Papadopoulos, “Automotive Disc Brake Squeal,” Journal of Sound and Vibration 267(1):105-166, 2003.

[3] R.T. Spurr, A theory of brake squeal, Proceedings of Automotive Division, Institution Mechanical Engineers (AD) Vol. 1, 1961, pp. 33–40.

[4] R.T. Spurr, "Brake squeal." Paper No. C95/71, Vibration and Noise in Motor Vehicles, I.Mech.E. 1971, pp 13 – 16.

[5] S.W.E. Earles, “A mechanism of disc-brake squeal”, Technical Report 770181, SAE, Warrendale, PA, 1977.

[6] N. Hoffmann, L. Gaul, “A sufficient criterion for the onset of sprag-slip oscillation”, Archive of Applied Mechanics 73 (2004) 650–660.

[7] J. Fieldhouse, N. Ashraf, C. Talbot, T. Pasquet, et al., “Measurement of the Dynamic Center of Pressure of a Brake Pad During a Braking Operation,” SAE Technical Paper 2006-01-3208, 2006.

[8] M.R. North, Disc brake squeal, in: Braking of Road Vehicles, Automobile Division of the Institution of Mechanical Engineers, Mechanical Engineering Publications Limited, London, England, 1976, pp. 169–176.

[9] N. Hoffmann, M. Fischer, R. Allgaier, L. Gaul, A minimal model for studying properties of the mode-coupling type instability in friction induced oscillations, Mechanics Research Communications, 29 (2002) 197-205.

[10] F. Cantone, F. Massi, A numerical investigation into the squeal instability: Effect of damping, Mechanical Systems and Signal Processing, Volume 25, Issue 5, 2011, Pages 1727-1737.

[11] W.V. Nack, Brake squeal analysis by finite elements, International Journal of Vehicle Design 23 (3–4) (2000) 263–275.

[12] F. Chen, D. Mckillip, J. Luo, and S. Wu, “Measurement and Analysis of Rotor In-plane Mode Induced Disc Brake Squeal and Beyond,” SAE Technical Paper 2004-01-2798, 2004, doi:10.4271/2004-01-2798.

[13] C. Park, M. Han, et al., "A Study on the Reduction of Disc Brake Squeal Using Complex Eigenvalue Analysis," SAE Technical Paper 2001-01-3141, 2001.

[14] A. Papinniemi, J. Zhao, D. Stanef, and J. Ding, “An Investigation of In-Plane Vibration Modes in Disc Brake Squeal Noise,” SAE Technical Paper 2005-01-3923, 2005, doi:10.4271/2005-01-3923.

[15] J. Park, J. C. Lee, S. Cho and K. Yoon, Reduction of Brake Squeal Analyzed in Terms of Coupling Between In-Plane and Out-of-Plane Modes. SAE Int. J. Passeng. Cars - Mech. Syst. 5(4), 2012, pp.1230-1243.

[16] T. Yokoyama et al, “A Study of Reduction for Brake Squeal in Disc In-Plane Mode”, SAE Technical Paper 2012-01-1825, 2012.

[17] M. Matsuzaki, “Brake Noise Caused by Longitudinal Vibration of the Disc Rotor”, SAE Technical Paper 930804.

[18] P. A. Meehan, A. C. Leslie, On the mechanisms, growth, amplitude and mitigation of brake squeal noise, Mechanical Systems and Signal Processing, Volume 152, 2021, 107469.

[19] F. Massi, L. Baillet, O. Giannini, A. Sestieri, Brake squeal: Linear and nonlinear numerical approaches, Mechanical Systems and Signal Processing,Volume 21, Issue 6, 2007, Pages 2374-2393.

[20] J. Kim, J. Kim, Y. Kim, W. Jeong, et al., "An Improvement of Brake Squeal CAE Model Considering Dynamic Contact Pressure Distribution," SAE Int. J. Passeng. Cars - Mech. Syst. 8(4),2015 (SAE Technical Paper 2015-01-2691).

[21] N. Hoffmann, L. Gaul, Effects of damping on mode-coupling instability in friction induced oscillations, ZAMM Z. Angew. Math. Mech. 83(8) (2003) 524-534.

[22] A. Akay, O. Giannini, F. Massi, A. Sestieri, “Disc brake squeal characterization through simplified test rigs”, Mechanical Systems and Signal Processing,Volume 23, Issue 8, 2009, Pages 2590–2607

[23] P. A. Meehan, Prediction of Wheel Squeal Noise under Mode Coupling, Journal of Sound and Vibration. 465 (2020) 115025.

[24] M Eriksson and S Jacobson, Friction behaviour and squeal generation of disc brakes at low speeds, Proc Instn Mech Engrs 215(D) (2001) 1245–1256.

[25] S. Oberst, J.C.S. Lai, Chaos in brake squeal noise, Journal of Sound and Vibration, Volume 330, Issue 5, 2011, Pages 955-975.

[26] B. Feeny, F.C. Moon, Chaos in a Forced Dry-Friction Oscillator: Experiments and Numerical Modelling, Journal of Sound and Vibration, Volume 170, Issue 3, 1994, Pages 303-323.

[27] P.A. Meehan, X. Liu: Modelling and mitigation of wheel squeal noise amplitude, Journal of Sound and Vibration, 413 (2018) 144–158.

[28] M. Stender, M. Tiedemann, N. Hoffmann, Energy harvesting below the onset of flutter, Journal of Sound and Vibration, Vol. 458, 2019, Pages 17-21.

[29] K.L. Johnson, Contact Mechanics, Cambridge University Press, Cambridge, 1985.

[30] Pohrt, R., Popov, V. Contact stiffness of randomly rough surfaces. Sci Rep 3, 3293 (2013).

[31] Meehan, P.A. Investigation of chaotic instabilities in railway wheel squeal. *Nonlinear Dyn* **100,** 159–172 (2020).

[32] J.M.T. Thompson, A.R. Bokaian, R. Ghaffari, Subharmonic resonances and chaotic motions of a bilinear oscillator, IMA Journal of Applied Mathematics, 31 (1983), pp. 207-234

[33] R. A. Ibrahim, Friction-Induced Vibration, Chatter, Squeal, and Chaos—Part II: Dynamics and Modeling, Appl. Mech. Rev. Jul 1994, 47(7): 227-253.
[34] F. C. Moon, Chaotic and Fractal Dynamics: An Introduction for Applied Scientists and Engineers, Wiley Interscience, 1992.
[35] P. van der Kloet and F. Neerhoff, Dynamic eigenvalues and Lyapunov exponents for nonlinear circuits, Proc. 2003 Workshop on Nonlinear Dynamics of Electronic Systems (NDES 2003) (2003) pp. 287–290.
[36] K. Shin, M.J. Brennan, J.-E. Oh, C.J. Harris, Analysis Of Disc Brake Noise Using A Two-Degree-Of-Freedom Model, Journal of Sound and Vibration, Volume 254, Issue 5, 2002, Pages 837-848.
[37] K. Shin, J. Oh, M. J. Brennan, Nonlinear Analysis of Friction Induced Vibrations of a Two-degree-of-freedom Model for Disc Brake Squeal Noise, JSME International Journal Series C Mechanical Systems, Machine Elements and Manufacturing, 2002, Volume 45, Issue 2, Pages 426-432.
[38] B. Lin, S. Chang, J. Hu, Y. Lue, Controlling chaos for automotive disc brake squeal suppression, Journal of Mechanical Science and Technology, 29(6), 2015, 2313 – 2322.
[39] S. Oberst, J.C.S. Lai, A statistical approach to estimate the Lyapunov spectrum in disc brake squeal, Journal of Sound and Vibration, Volume 334, 2015, Pages 120-135.
[40] S. Oberst, J.C.S. Lai, Nonlinear transient and chaotic interactions in disc brake squeal, Journal of Sound and Vibration, Volume 342, 2015, Pages 272-289.
[41] B.F. Feeny, F.C. Moon, Quenching Stick–Slip Chaos With Dither, Journal of Sound and Vibration, Volume 237, Issue 1, 2000, Pages 173-180.
[42] A. Wolf, J. B. Swift, H. L. Swinney, J. A. Vastano, Determining Lyapunov exponents from a time series, Physica D: Nonlinear Phenomena, Volume 16, Issue 3, 1985, Pages 285-317.

Figures

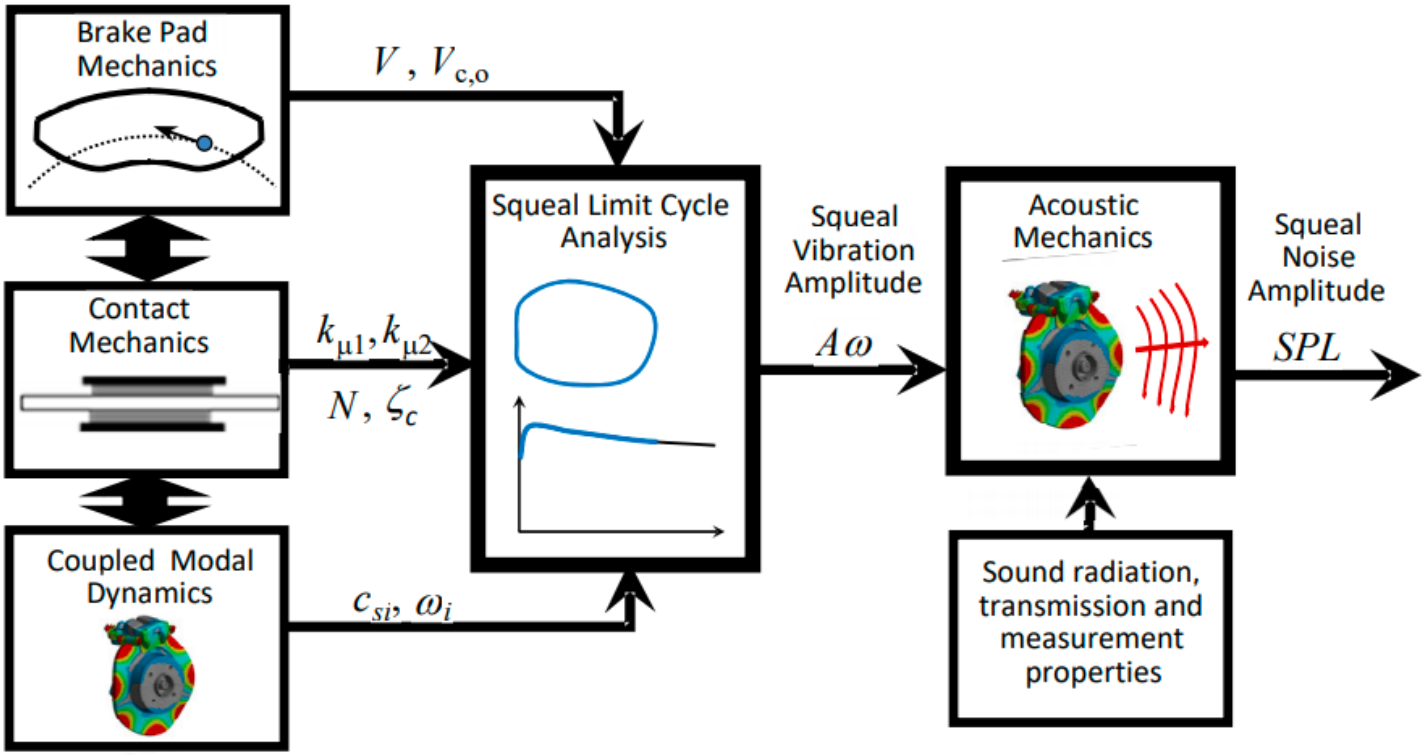

Figure 1

Please see the Manuscript PDF file for the complete figure caption

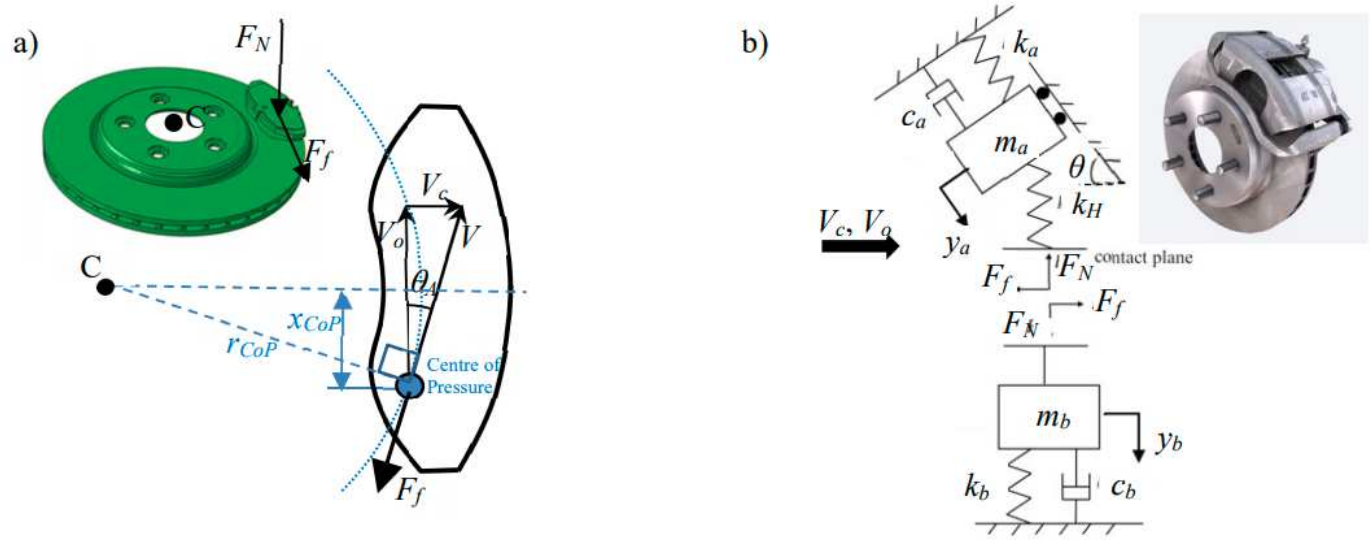

Figure 2

Please see the Manuscript PDF file for the complete figure caption

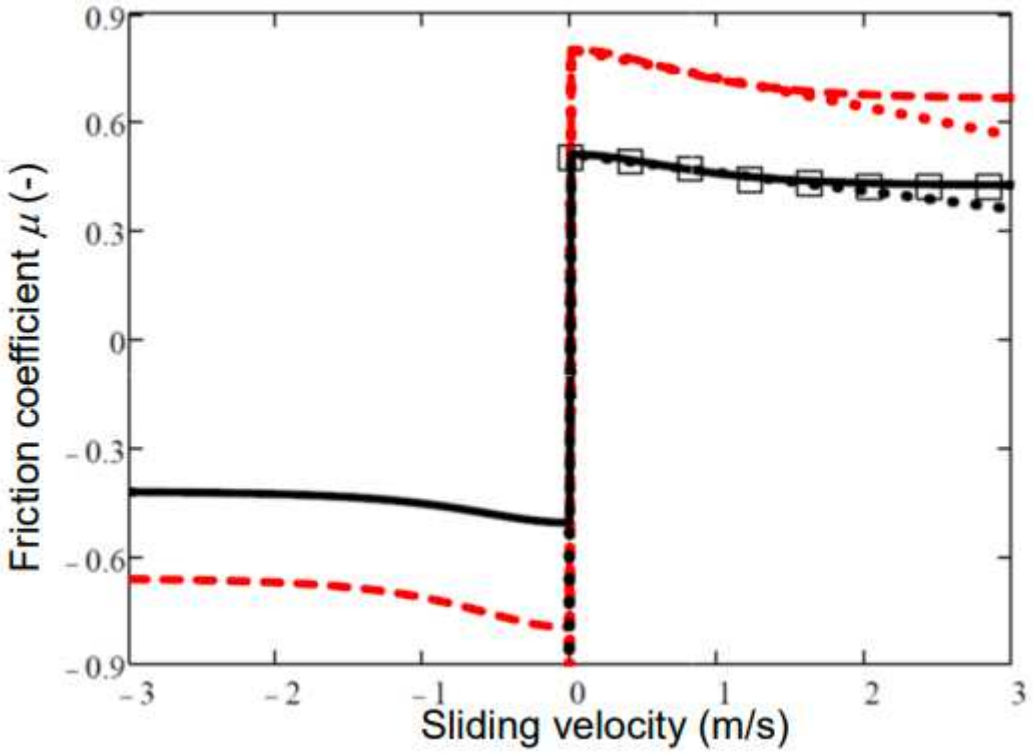

Figure 3

Please see the Manuscript PDF file for the complete figure caption

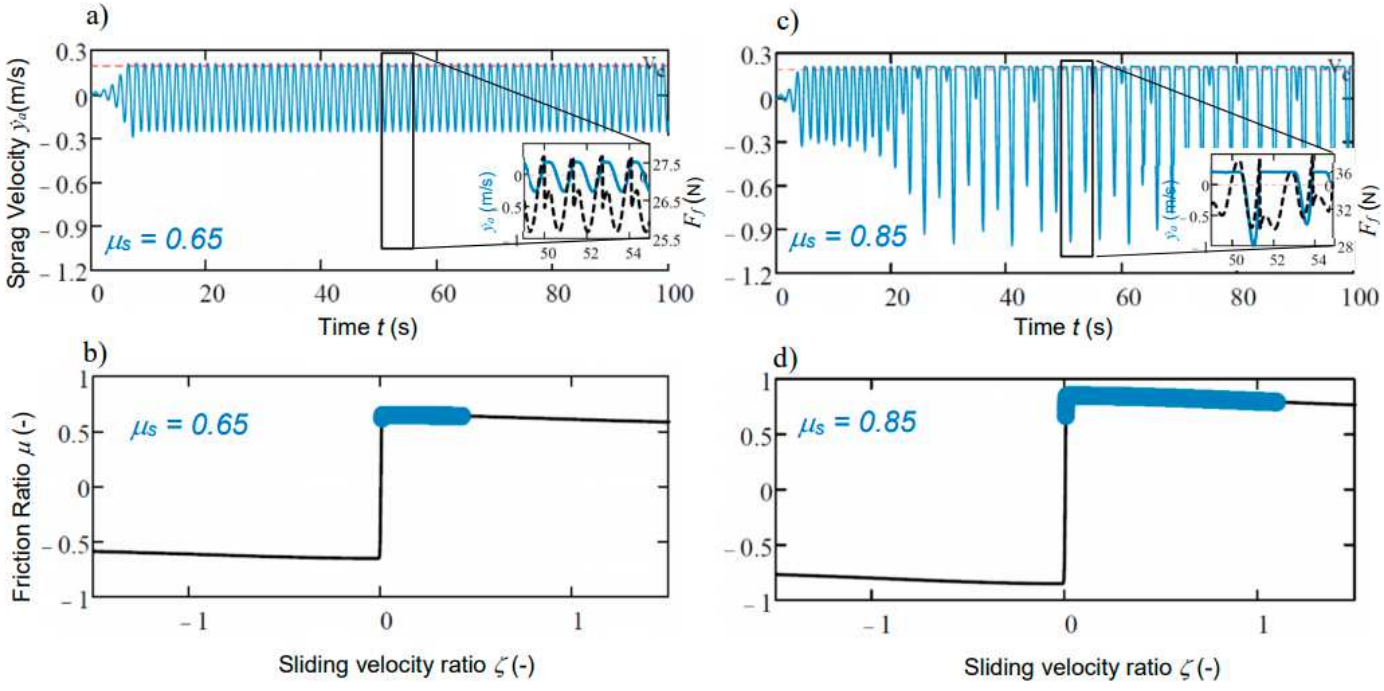

Figure 4

Please see the Manuscript PDF file for the complete figure caption

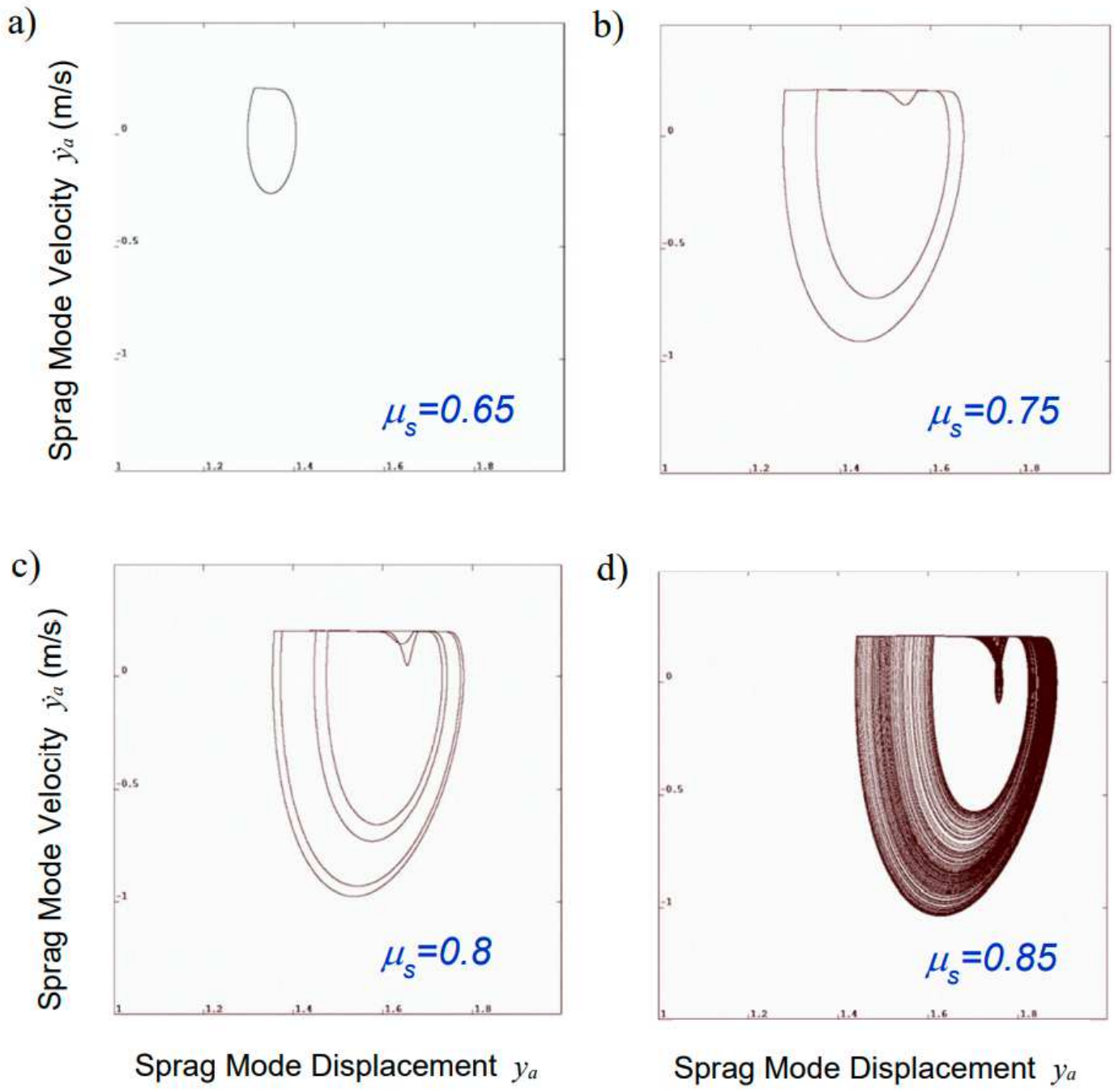

Figure 5

Please see the Manuscript PDF file for the complete figure caption

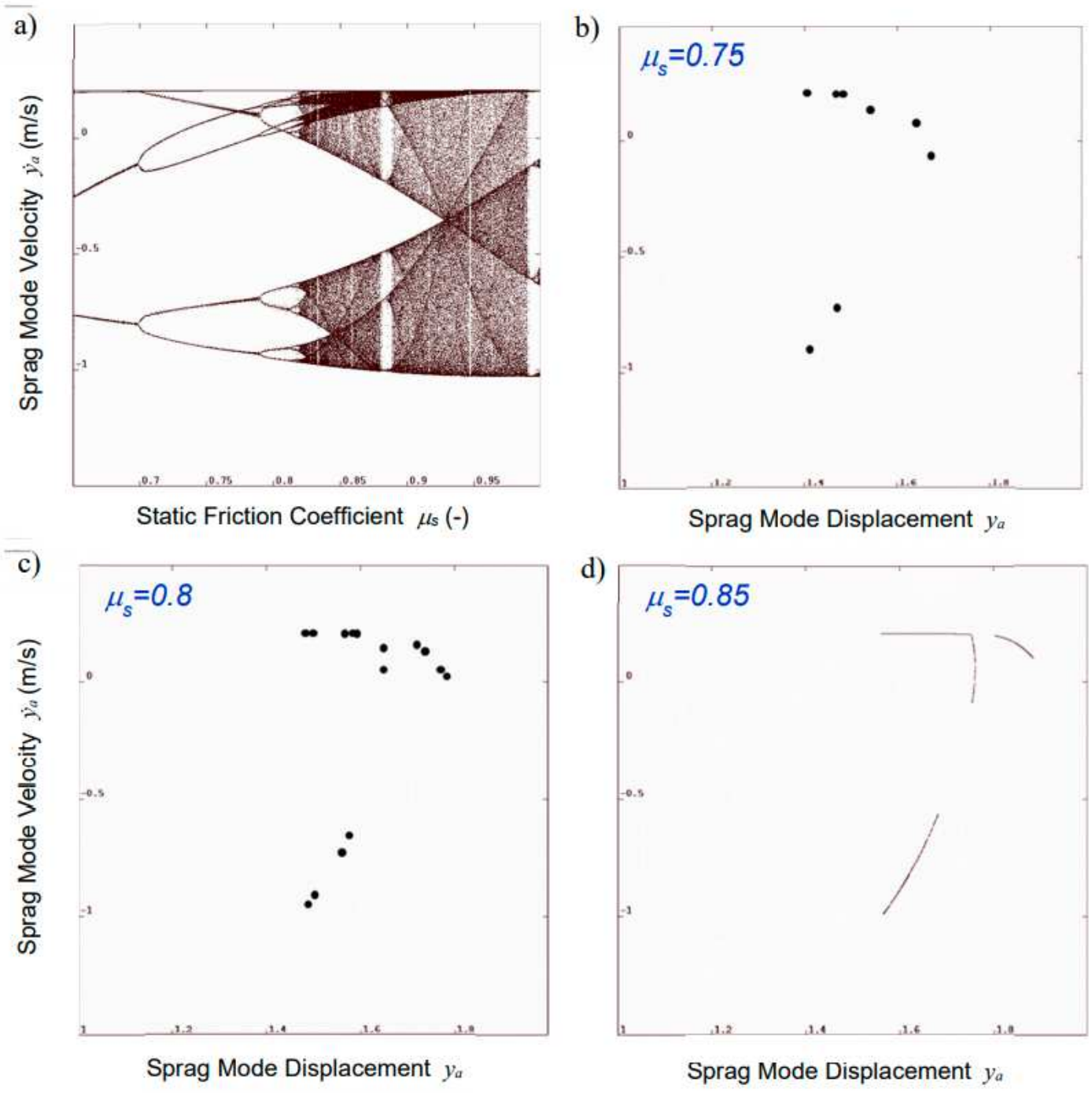

Figure 6

Please see the Manuscript PDF file for the complete figure caption

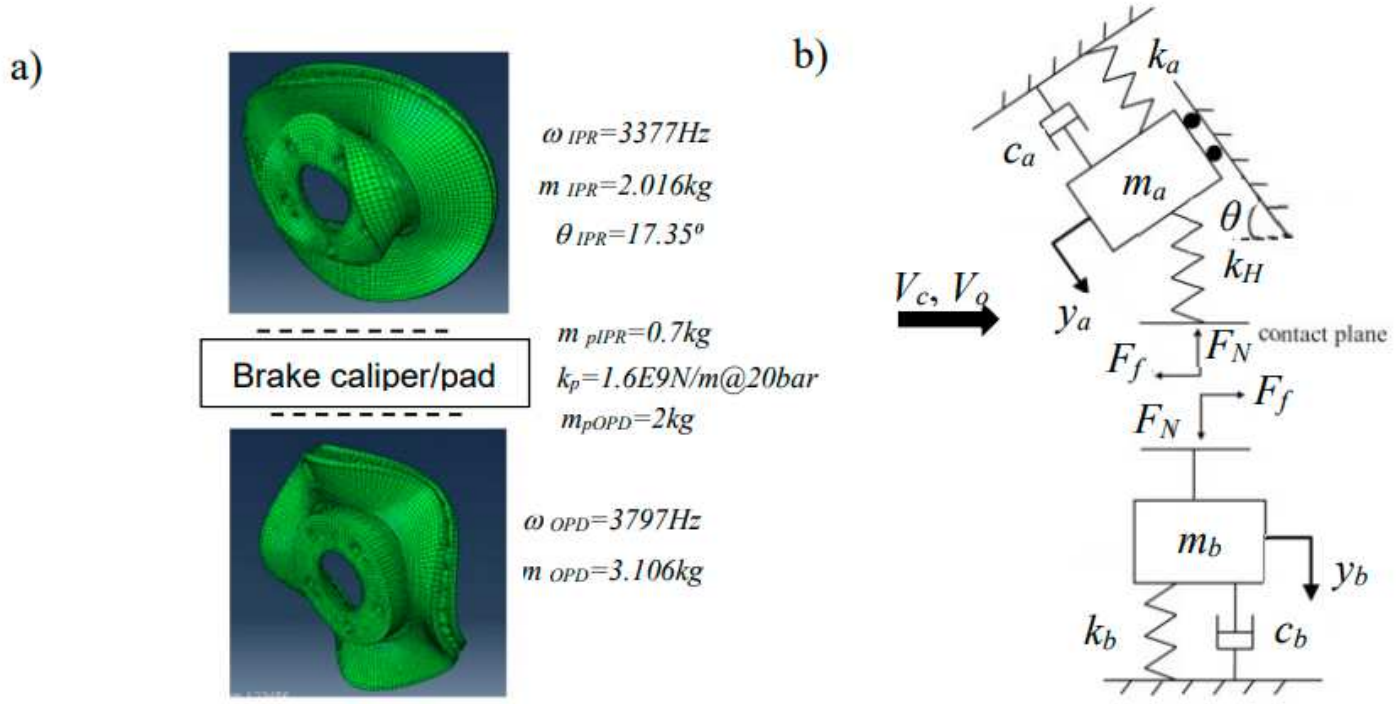

Figure 7

Please see the Manuscript PDF file for the complete figure caption

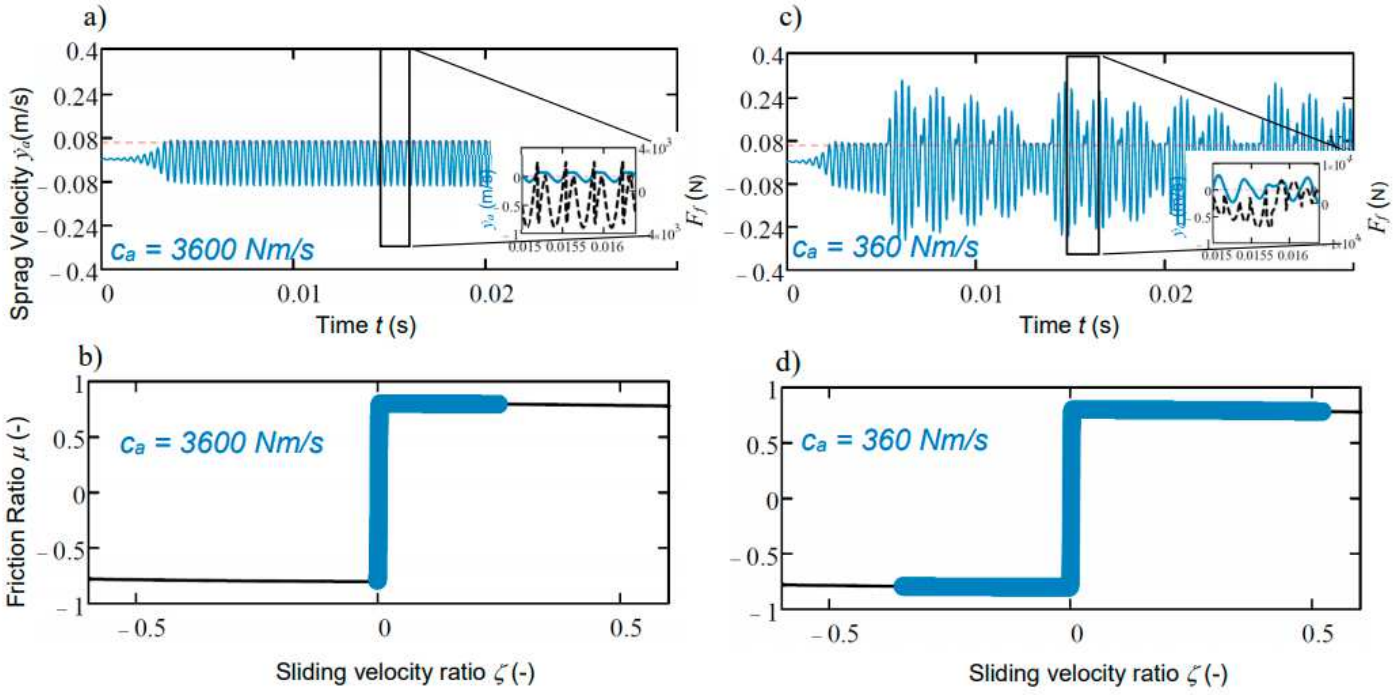

Figure 8

Please see the Manuscript PDF file for the complete figure caption

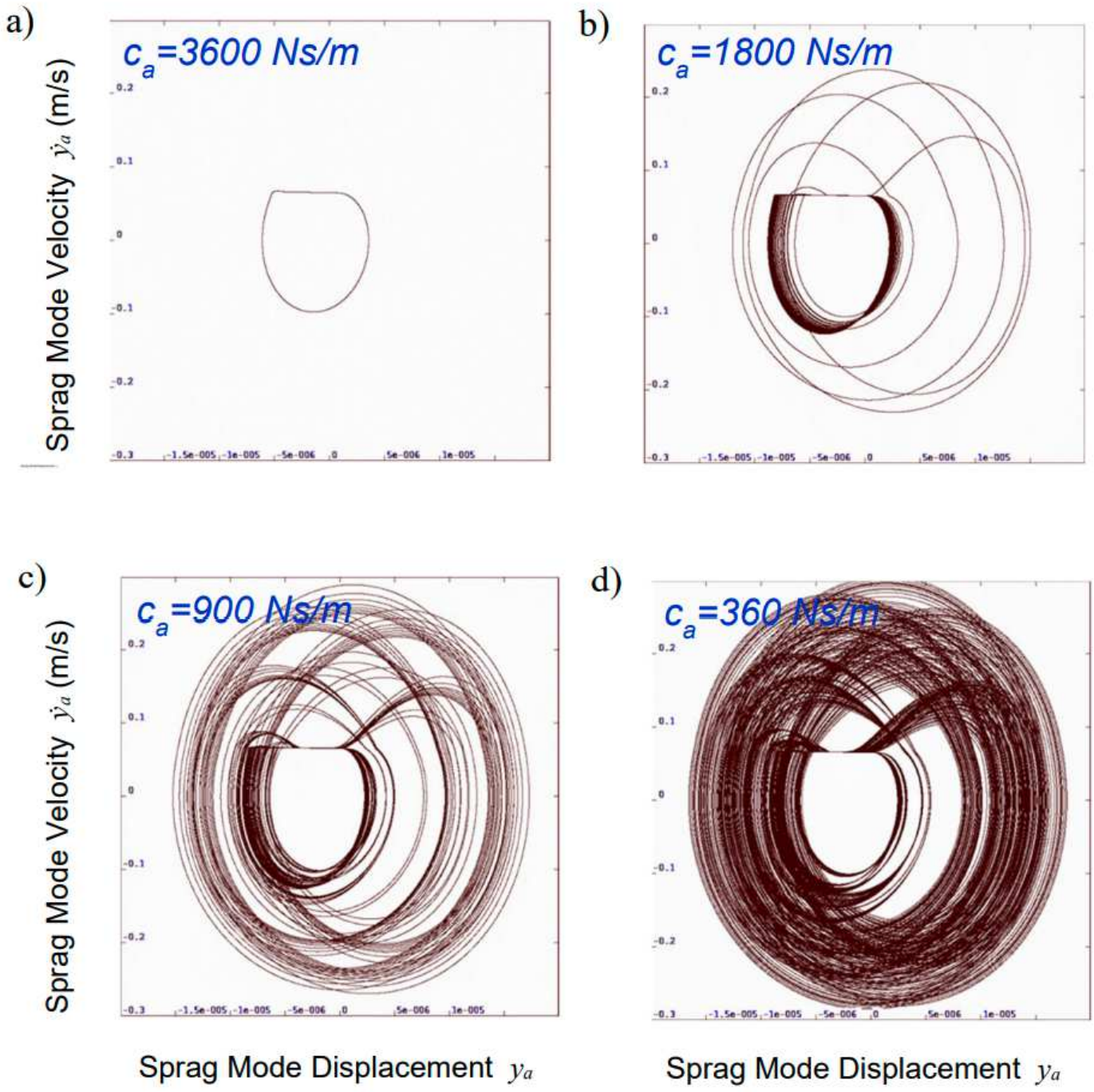

Figure 9

Please see the Manuscript PDF file for the complete figure caption

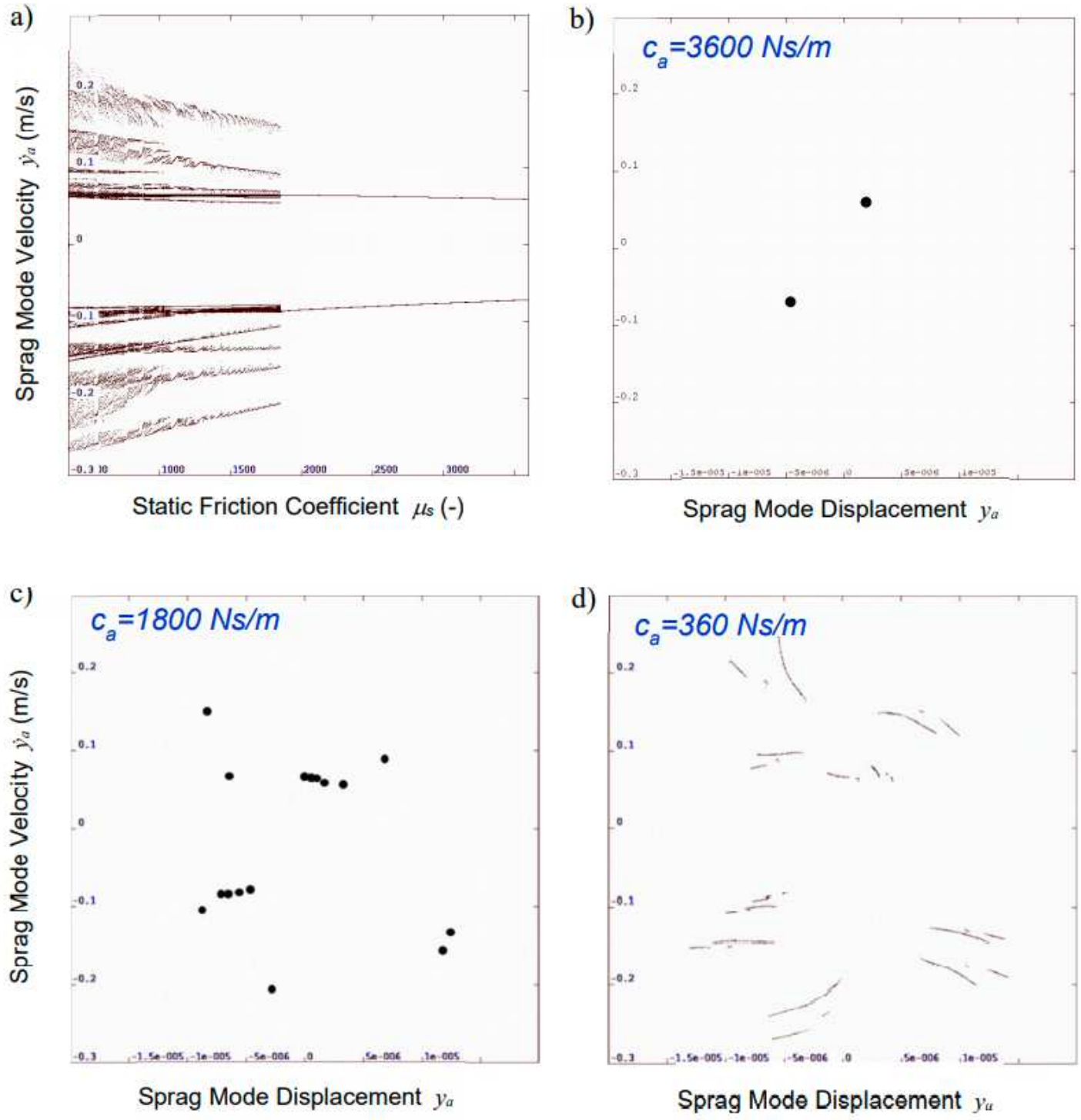

Figure 10

Please see the Manuscript PDF file for the complete figure caption

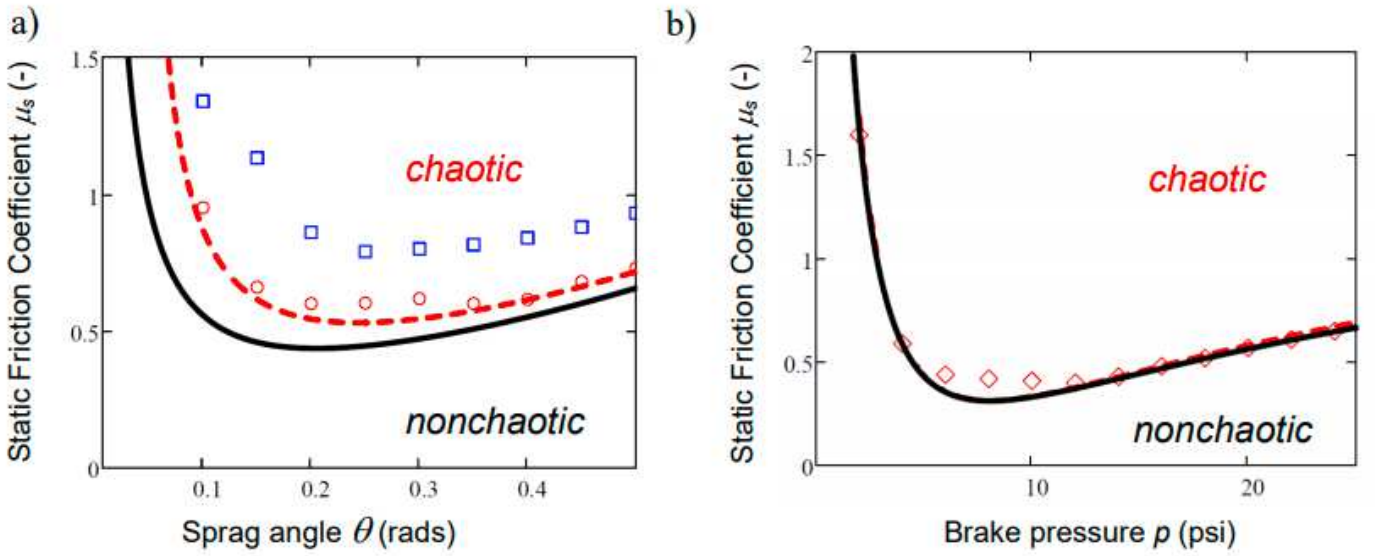

Figure 11

Please see the Manuscript PDF file for the complete figure caption